SCHOOL OF MATHEMATICAL & COMPUTER SCIENCES

DEPARTMENT OF MATHEMATICS

COURSEWORK SUBMISSION

Please complete all of the following:

Programme	MSC Applied mathematical sc with climate change impact modelling
Year of Study	2019/2020
Surname	Ajayi
First Name	Olayinka Josiah
Matriculation No	H00328625
Course Code	F11GM
Course Title	Masters Project and Dissertation
Title of Assignment	Particle Trajectory in Solid-body Vortex and Source-sink Pair Flow Fields Using the Maxey-Riley Equation.
Lecturer	Dr Cathal Cummins and Dr Simon Malham
Date of Submission	14th July, 2020.

You must complete the course title and course code or your Coursework will be returned. Please submit coursework into the Mathematics coursework box by 3.30pm.

I affirm that this assignment is my sole and original work, and that any assistance I receive with the development of this work is acknowledged on page one.	**Signed** 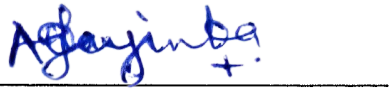 **Dated** 14th July, 2020.

Particle Trajectory in Solid-body Vortex and Source-sink Pair Flow Fields Using the Maxey-Riley Equation

Olayinka Josiah Ajayi
H00328625

Supervisor: Dr Cathal Cummins
Second supervisor: Dr Simon Malham
July 14, 2020

Declaration

I, Olayinka Josiah Ajayi, confirm that this work submitted for assessment is my own and is expressed in my words. Any uses made within it of the works of other authors in any form e.g. ideas, equations, figures, text, tables, programs, are properly acknowledged at any point of their use. A list of references employed is included.

Signature 

Acknowldegement

I acknowledge the support of God almighty, for giving me the necessary inspiration to tackle the challenges I encountered, and for allowing me enjoy good health all through the period of my dissertation. I wish to thank the Commonwealth Scholarship Commission for the opportunity to undertake this masters programme here at Heriot-Watt; without their funding this current reality would be impossible.

My appreciation goes to my supervisor Dr Cathal for the support he gave all through the dissertation. His corrections and opinions helped shape this dissertation into its current form.

Also, my appreciation goes to my lovely mother Mrs Gloria Ajayi (*Iya Funmi*) for nuturing me through the years; without her love and drive, my siblings and I would not have made it this far. And to my awesome mentor and mother, Mrs Ronke Ogundimu (*Class Teacher*) for her prayers and moral support during this period and since the first day she came into my life. With her help over the years, I have been able to pursue my dreams and have achieved them. And finally, to the love of my life, Motunrayo mi (*my pepperoni pizza*) for her love and encouragement (not leaving out her jokes) during this period, as it helped me maintain sound mental health and killed the boredom that resulted from the lockdown due to the COVID-19 pandemic. Thank you Motun, for loving me regardless of my flaws.

Abstract

The question of how a particle moves in a fluid is the primary focus of this dissertation. The flow fields of interest are solid-body vortex and source-sink pair. Experiments reveal that buoyant particles would act as fluid tracers by following the fluid at each point with equal velocity. But for a particle with density greater (or lesser) than that of the fluid, the answer is not glaring for both flow fields of interest. For this, the Maxey-Riley equation is introduced, which describes the motion of particles in a fluid and is used to answer the above question.

A mathematical model for an aerosol extractor (from COVID-19 patients) is designed using the solution of the Maxey-Riley equation for a source-sink pair flow field. And the effect of gravity on the aerosol extractor is considered alongside the effect of a constant flow stream.

Contents

Chapter 1

Introduction

How would a particle of density slightly greater/less than (or equal to) the fluid move when immersed in the fluid of a certain flow field? This question of how a particle would move in a fluid has been of great interest to the community of researchers in fluid mechanics. For a buoyant particle (equal density with the fluid) present in a fluid experiencing a steady flow, it would act as a fluid tracer, that is, it would follow the fluid and have the same velocity as the fluid (over time) at the current position. So, for a particle with greater density, would it just remain static at that position or lag compared to the flow. And would a particle of lesser density act just like a buoyant particle?

These were some of the question Tchen tried answering in his 1947 PhD thesis on the motion of a spherical particle in a fluid [25]. A particle immersed in a fluid is acted upon by several forces, which induces motion—according to Newton's law of motion. Tchen attempted to describe these forces in his thesis, but unfortunately failed to properly account for all the forces acting on the particle, and the terms he used to express the forces accounted for, contained a number of errors [14]. Other researchers went ahead to correct several of the terms Tchen had in his equation, meanwhile many literatures have based their research on the validity of Tchen's equation [17]. Then in 1983 Maxey and Riley chose to derive the equation governing the motion of a spherical particle in a fluid from first principle. This approach was taken to correct the errors made by Tchen [14].
The equation derived by Maxey and Riley [14] is an elaboration of the classical Newton's equation of motion

$$F \;=\; ma \;. \tag{1.1}$$

Where the equation represents the forces (F) acting on a body of mass m with an acceleration a. According to Maxey and Riley [14], the forces acting on a particle in a fluid are the fluid pressure gradient, buoyancy, drag force, added mass and the Basset's history/augmented viscous drag. These forces combine in the form given

below

$$\text{Force} = \textbf{Fluid pressure gradient} + \textbf{Buoyancy} + \textbf{Drag force} + \textbf{Added mass} + \textbf{Basset history}$$

$$m_p' \frac{\mathrm{d}\boldsymbol{V'}}{\mathrm{d}\tau'} = m_f' \frac{\mathrm{D}\boldsymbol{U'}}{\mathrm{D}\tau'} + \left(m_p' - m_f'\right)\boldsymbol{g'} + 6\pi a'\mu' \left[\boldsymbol{U'} - \boldsymbol{V'} + \frac{a'^2}{6}\Delta\boldsymbol{U'}\right] - \frac{m_f'}{2}\left[\frac{\mathrm{d}\boldsymbol{V'}}{\mathrm{d}\tau'} - \frac{\mathrm{D}}{\mathrm{D}\tau'}\left(\boldsymbol{U'} + \frac{a'^2}{10}\Delta\boldsymbol{U'}\right)\right] + \int_0^{\tau'} \frac{1}{\sqrt{\tau' - s'}} \frac{\mathrm{d}}{\mathrm{d}s'}\left[\boldsymbol{U'} - \boldsymbol{V'} + \frac{a'^2}{6}\Delta\boldsymbol{U'}\right] \mathrm{d}s', \tag{1.2}$$

where,

$m_p' \equiv$ particle mass; $m_f' \equiv$ fluid mass; $\boldsymbol{U'} \equiv$ fluid velocity; $\boldsymbol{V'} \equiv$ particle velocity, $\mu' \equiv$ dynamic viscosity; $\boldsymbol{g'} \equiv$ gravity; $a' \equiv$ particle radius; $\tau', s' \equiv$ time variables; and $\Delta \equiv$ Laplacian operator.

The Maxey-Riley equation [14] describes the motion of a finite-sized spherical particle in a non-quiescence fluid flow. The equation takes the form of a second order, implicit integro-differential equation with a singular kernel, and with a forcing term that explodes at starting time [9]. The equation is seldom used in most literatures in the above form due to the presence of the history term which make it an integro-differential and makes it more difficult to solve.

Many researchers introduce the Maxey-Riley equation in their problem of interest without the history term, and several justifications has been given as to why this term has been neglected. Some of the authors of the ASME symposium showed that by using dimensional parameters, and with the assumption that the particle moved in a quasistatic manner, the history and added mass term do not have any significant influence to the quantities they were interested in, which are mostly time-averaged properties of the fluid in motion [17]. Since the transient terms changes sign frequently, the total effect of these terms become very small compared to the Stokes drag term which has a significant effect [17].

Although in the case of less dense particles, for example bubbly and slurry flows, the Basset's history terms accounts for a quarter of the instantaneous force on a spherical particle when the ratio of fluid to particle density is greater than 1.5, since now the desired result is an instantaneous and not a time-averaged quantity [17]. This led to the resolve that the Basset's term and added mass term be included in any equation of motion where the density ratio is greater than 1[17].

The inclusion of the transient terms—particularly the history term—increases the computer memory required for numerically computing the solution to the Maxey-Riley equation—the trajectory of the sphere. This is due to the integral term added by the Basset's history, which makes the problem a nonlocal one. Also, if a Lagrangian simulation of ensembles of spherical particles are considered, the inclusion of the Basset's term slows the computation significantly [17, 19]. Researchers in previous

years never did attempt for an analytical solution of the Maxey-Riley equation due to its integro-differential form. Even for a numerical solution, including the history term results in more storage requirement which increases with time [19].

Michaelides provided a new approach to solving the Maxey-Riley equation with the inclusion of the Basset's history term [16]. The approach involves a transformation of the equation of motion of a spherical particle in a fluid, where the velocity of the particle is nonexistent in the Basset's term integral. The resulting second-order ODE is explicit in the dependent variable and save computation time and significantly reduces memory requirements.

The Maxey-Riley equation was used as a forced, time-dependent Robin boundary condition of the 1-dimensional diffusion equation [19]. The solution was applied to several physical situations, and it was observed that the effect of the Basset's history term was noted to affect the decay rate of the solution. And for a particle settling under gravity, the particle relaxes slowly to its terminal velocity, whereas relaxation would occur exponentially fast if the history term were ignored. Observation showed that the growth rate of a raindrop can be utterly miscalculated when history effects are not taken into consideration [19].

Maxey studied the motion of particles in a fluid settling under gravity, under the influence of Stokes drag, through an infinite oscillatory cellular flow field. He considered the responses of aerosol which are denser that the surrounding fluid, and bubbles which are of lesser density [15]. The Maxey-Riley equation [14] was used to model the motion of particles, neglecting the history term since computational test shows it to be less significant in the results. Candelier showed that the history term is of significance for a particle placed in a rotating fluid [4]. They showed that the rotating fluid influences the ejection rate of a particle; they showed this by dropping a denser particle, compared to the fluid, at the centre of a solid-body vortex. Measurement showed that the calculation without the history term increased the ejection rate by 10%. Sudarsanam affirms that the Basset's history term is of significance for particles experiencing rapid acceleration and when the particle is certain to revisit a position numerous times in a session [23]. In addition, if the characteristic length is much larger than the radius of the particle, the Faxen's correction terms can be neglected as this effect would be insignificant over large distance as compared to the particle radius.

The history term is shown to be of significance in the solution of the Maxey-Riley equation. The solution to the Maxey-Riley equation is rather an algebraic decay to an asymptotic state, as opposed to the exponential convergence that is observed when the Basset term is neglected [12]. It was proved that the algebraic decay is a universal property of the Maxey-Riley equation, and a proof for the existence and uniqueness of global solution to the equation was provided [12].

Research was conducted on the dispersion of heavy particles in an isolated pancake-like vortex [10]. This was achieved by substituting the velocity field for a pancake vortex into the Maxey-Riley equation and solved numerically. A low particle concentration was assumed so that particle to particle interactions as well as the action of particles on the flow itself can be neglected. Based on this assumption and as suggested by

Raju [20], the added mass and history terms can be neglected, as they would have no significant effect in their result. With this, it was observed that the particles denser than the neighboring fluid drifted away from the focus of the vortex.

Bergougnoux used particle image-velocimetry to model the settling of particle through a vortical structure, induced by gravity at low Stokes number [3]. They compared this measurement with numerical forecasts from the solution to the equation proposed by Maxey[15]. They added that the history term is meant to describe rapid acceleration, which was not of relevance to their experiment.

Monroy used a variation of the Maxey-Riley equation [14]—the Maxey-Riley-Gatignol equation—in modelling the dynamics of sinking biogenic particles in the ocean [21]. Their purpose was to portray an application of the novel equation in oceanographic framework. The Faxen's correction term together with the history term were neglected since the particles considered are significantly small, but not negligible, and with high kinetic viscosity which makes the effect of these terms negligible.

Chong conducted a research on how particles in a viscous stream can be trapped, transported, and focused [6]. The streaming flow was obtained from past work and the ensuing velocity field was used together with the Maxey-Riley equation [14] to find the trajectory of the particle. The Maxey-Riley equation used ignored the effect of gravity, but included the effect of the Faxen's correction terms, as their effect are noticeable in the regions of high vorticity, where the particle stays for prolonged time during motion. The Basset's history term which characterizes the aggregate effect of the dispersion of vorticity from the particle for the period of traveling [26] was also included in the equation which made the solution much more complex to solve.

The feeding mechanism of *Aurelia aurita* (jelly fish) was studied by Costello and Colin, and their findings showed that *A. aurita* was not a generalist predator but rather a selective one [7]. The selection was observed to be a function of the diameter of the *A. aurita* bell and the escape velocity of the zooplankton around the flow field of the of the medusae. The prey is captured by the rhythmic movements of the bell of the medusae, and this causes the prey to be entrained in the flow field of the medusae and it is positively selected [7]. Peng and Dabiri used the Maxey-Riley equation to model the movement of zooplanktons such as the copepod in the flow field generated by the movement of the bell-shaped dome of the swimming Aurelia aurita in a pond [18]. This study was to find the region over which the velocity field of the swimming *A. aurita* is felt, which would define the capture region for zooplanktons.

Chapter 2

Finding the particle trajectory in a solid-body vortex

The question asked in the introduction would now be answered in this section. The question is now slightly tweaked as: where would the bubbles in a cup of tea go when stirred? This is equivalent to finding the trajectory of a particle of lesser density (than the fluid) placed in a fluid with a solid-body vortex flow field. This was presented in the paper by Raju and Meiburg [20]. Some of the result obtained would be repeated here to answer the above question. The approach to be taken would involve substituting the solid-body vortex velocity flow field into the Maxey-Riley equation and then solving numerically using MATLAB. The Basset history term is neglected for this scenario (and subsequent ones as well), as the overall effect of vorticity from the particle is assumed to be negligible. This reduces the Maxey-Riley equation (1.2) to

$$m_p' \frac{\mathrm{d}\boldsymbol{V'}}{\mathrm{d}\tau'} = m_f' \frac{\mathrm{D}\boldsymbol{U'}}{\mathrm{D}\tau'} + \left(m_p' - m_f'\right)\boldsymbol{g'} + 6\pi a'\mu' \left[\mathbf{U}' - \mathbf{V}' + \frac{a'^2}{6}\Delta\mathbf{U}'\right] - \frac{m_f'}{2}\left[\frac{\mathrm{d}\mathbf{V}'}{\mathrm{d}\tau'} - \frac{\mathrm{D}}{\mathrm{D}\tau'}\left(\mathbf{U}' + \frac{a'^2}{10}\Delta\mathbf{U}'\right)\right]. \tag{2.1}$$

Nondimensionalizing the above equation and bearing in mind that $\Delta\boldsymbol{U'} = 0$ for the solid-body vortex flow field, equation (2.1) yields

$$\frac{\mathrm{d}\boldsymbol{v}}{\mathrm{d}t} - \frac{3}{2}R\frac{\mathrm{D}\boldsymbol{u}}{\mathrm{D}t} = -A\left(\boldsymbol{v} - \boldsymbol{u}\right) + \left(1 - \frac{3}{2}R\right)\boldsymbol{g}, \tag{2.2}$$

where,

$$R = \frac{2\rho_f'}{\rho_f' + 2\rho_p'}, \quad A = \frac{R}{St}, \quad St = \frac{2}{9}\left(\frac{a'}{L'}\right)^2 Re, \quad Re = \frac{U'L'}{\nu'}, \quad \boldsymbol{v} = \frac{\boldsymbol{V'}}{U'},$$
$$\boldsymbol{u} = \frac{\boldsymbol{U'}}{U'}, \quad t = \frac{\tau' U'}{L'}, \quad \boldsymbol{g} = \frac{\boldsymbol{g'}L'}{U'^2}\ , \tag{2.3}$$

and

$R \equiv$ fluid to particle density ratio; $A \equiv$ Stokes drag coefficient; $St \equiv$ Stokes number; $Re \equiv$ Reynolds number; $\rho_f' \equiv$ fluid density; $\rho_p' \equiv$ particle density; $\nu' \equiv$ kinematic viscosity; $U' \equiv$ characteristic speed; and $L' \equiv$ characteristic length .

Before now, all parameters in this chapter were considered dimensional parameters. Having nondimensionalized, the nondimensional parameters are without a prime ($\prime$) floating at their top. The characteristic length (L') used for the problems relating to the solid-body vortex would be the maximum distance across the circular space, that is, the diameter. In the case of the tea problem, this would be the diameter of the teacup. It should be noted that every parameter still has the same meaning as before. The details of the nondimensionalization is provided in appendix A.

2.1 Converting to polar coordinates

The solid-body velocity flow field is a circular motion, and the traditional cartesian coordinate system would not be very useful in analyzing the solution of interest. The polar coordinate system is most suitable for a system involving circular motion, and this would come in handy in the analysis ahead.

Drawing from the paper by Raju and Meiburg[20], the velocity field vector for a solid-body vortex in cartesian coordinate system is

$$\boldsymbol{u} \;=\; \left(-\frac{\omega_0}{2}y\;,\frac{\omega_0}{2}x\;\right),$$

where ω_0 is the nondimensionalized angular velocity defined as $\omega_0 = \omega_0'/\alpha'$, and α' is the characteristic angular velocity, while ω_0' is the dimensional angular velocity.

Employing the transformation below to convert from cartesian to polar coordinate

$$\begin{bmatrix} u_r \\ u_\theta \end{bmatrix} = \begin{bmatrix} \cos\theta & \sin\theta \\ -\sin\theta & \cos\theta \end{bmatrix} \begin{bmatrix} u_x \\ u_y \end{bmatrix}, \tag{2.4}$$

the velocity field is transformed to

$$\boldsymbol{u} \;=\; \left(0\;,r\frac{\omega_0}{2}\;\right).$$

The terms in the reduced Maxey-Riley equation (2.2) are equally transformed to polar coordinate below

$$\frac{\mathrm{D}\boldsymbol{u}}{\mathrm{D}t} = \frac{\partial \boldsymbol{u}}{\partial t} + (\boldsymbol{u}\cdot\nabla)\,\boldsymbol{u}$$

$$\frac{\partial \boldsymbol{u}}{\partial t} = \frac{\partial u_\theta}{\partial t}\hat{e}_\theta = \frac{\omega_0}{2}\frac{\mathrm{d}r\,(t)}{\mathrm{d}t}\hat{e}_\theta$$

$$(\boldsymbol{u}\cdot\nabla)\,\boldsymbol{u} = \frac{\partial \boldsymbol{u}}{\partial r}\frac{\partial r}{\partial t} + \frac{\partial \boldsymbol{u}}{\partial \theta}\frac{\partial \theta}{\partial t}$$

$$= \frac{1}{r}u_\theta\frac{\partial \boldsymbol{u}}{\partial \theta} \;=\; \frac{u_\theta}{r}\left[-u_\theta\hat{e}_r \;+\; \frac{\partial u_\theta}{\partial \theta}\hat{e}_\theta\right] \;=\; \frac{r\omega_0}{2}\;\frac{1}{r}\left[-\frac{r\omega_0}{2}\right]\hat{e}_r = -\frac{r{\omega_0}^2}{4}\hat{e}_r$$

Therefore,

$$\frac{\mathrm{D}\boldsymbol{u}}{\mathrm{D}t} = -\frac{r{\omega_0}^2}{4}\hat{e}_r + \frac{\omega_0}{2}\frac{\mathrm{d}r\left(t\right)}{\mathrm{d}t}\hat{e}_\theta$$

The acceleration becomes

$$\frac{\mathrm{d}\boldsymbol{v}}{\mathrm{d}t} = \left(\frac{\mathrm{d}^2 r\left(t\right)}{\mathrm{d}t^2} - r\left(t\right)\left[\frac{\mathrm{d}\theta\left(t\right)}{\mathrm{d}t}\right]^2\right)\hat{e}_r + \left(2\frac{\mathrm{d}r\left(t\right)}{\mathrm{d}t}\frac{\mathrm{d}\theta\left(t\right)}{\mathrm{d}t} + r\left(t\right)\frac{\mathrm{d}^2\theta\left(t\right)}{\mathrm{d}t^2}\right)\hat{e}_\theta \ , \quad (2.5)$$

and

$$\boldsymbol{v} = \frac{\mathrm{d}r\left(t\right)}{\mathrm{d}t}\hat{e}_r + r\left(t\right)\frac{\mathrm{d}\theta\left(t\right)}{\mathrm{d}t}\hat{e}_\theta \ . \quad (2.6)$$

The components of the nondimensionalized Maxey-Riley equation in polar form is given as

$$\frac{\mathrm{d}^2 r\left(t\right)}{\mathrm{d}t^2} - r\left(t\right)\left[\frac{\mathrm{d}\theta\left(t\right)}{\mathrm{d}t}\right]^2 + \frac{3}{8}R{\omega_0}^2 r\left(t\right) + A\frac{\mathrm{d}r\left(t\right)}{\mathrm{d}t} = 0 \quad (2.7)$$

$$r\left(t\right)\frac{\mathrm{d}^2\theta\left(t\right)}{\mathrm{d}t^2} + 2\frac{\mathrm{d}r\left(t\right)}{\mathrm{d}t}\frac{\mathrm{d}\theta\left(t\right)}{\mathrm{d}t} - \frac{3}{4}R\omega_0\frac{\mathrm{d}r\left(t\right)}{\mathrm{d}t} + Ar\left(t\right)\frac{\mathrm{d}\theta\left(t\right)}{\mathrm{d}t} - A\frac{\omega_0}{2}r\left(t\right) = 0 \ . \quad (2.8)$$

It should be noted that the effect of gravity is neglected for this problem.

2.2 Answer to the tea question

Consider a bubble with radius 1 mm and density $1.4\,\mathrm{kg/m^3}$ [22] floating on a tea of density $971.82\,\mathrm{kg/m^3}$ in a teacup 15 cm wide. The kinematic viscosity of water is $4.13 \times 10^{-7}\,\mathrm{m^2 s^{-1}}$ [1]. All parameters are given at 71.1 °C. Since the bubble is formed inside the tea, it is assumed that the tea is at rest, therefore giving the bubble an initial angular velocity of $0\,\mathrm{rad.s^{-1}}$ and radial velocity of $0\,\mathrm{ms^{-1}}$. It is assumed that a bubble completes 1 revolution in an average of 2 seconds, so the characteristic angular velocity (α') is taken as $\pi\,\mathrm{rad.s^{-1}}$, and the characteristic linear velocity (U') can be obtained using $U' = \alpha' L'/2$. Given that the bubble is formed close to the wall of the teacup, the trajectory of the bubble when the tea is stirred at a speed of $0.2\pi\,\mathrm{rads.s^{-1}}$ is captured with the nondimensional parameters below

$$A = 2.36, \quad R = 1.99, \quad \omega_0 = 0.2, \quad St = 0.846, \quad Re = 8.56 \times 10^4 \ .$$

The graph below shows the trajectory of a bubble starting from rest at the edge of the teacup and swirling towards the centre.

The bubble picks up momentum and gradually spirals towards the centre of the teacup, with an increasing radial velocity (Figure 2.2a). The radial velocity is maintained briefly for an interval of time and then reduces with time, approaching 0 as it reaches the centre of the teacup (Figure 2.2b). The angular velocity increases with time and is maintained when it equals that of the fluid (tea) (Figure 2.2a and 2.2b). This result answers the question previously asked at the beginning of this section.

The equation also provides an answer for a particle with density greater than the fluid. For this, consider a ball of radius 12 mm and with a density of $1000\,\mathrm{kg/m^3}$ immersed

in a pool of sunflower oil, 10 m in diameter with a density of 917 kg/m^3 [8]. The kinematic viscosity of sunflower oil is 5.8×10^{-5} m^{2}s^{-1} [8]. All parameters are given at room temperature. It is assumed that the ball completes 1 revolution in an average of 20 seconds, so the characteristic angular velocity (α') is taken as $\pi/10$ rad.s^{-1}, and the characteristic linear velocity (U') can be obtained using $U' = \alpha' L'/2$.. If the ball is placed a distance of 1 m from the centre of the pool, and the pool is stirred at a speed of 0.6π rad.s^{-1}, the nondimensional parameters capturing these parameters are

$$A = 7.25, \quad R = 0.63, \quad \omega_0 = 6, \quad St = 0.087, \quad Re = 2.71 \times 10^5 \ .$$

The trajectory for the ball is seen in Figure 2.3.

The ball commences its journey by briefly moving inwards as seen in the radial velocity (Figure 2.4b). This event is immediately followed by the ball spiraling outwards with an increased radial velocity. The radial velocity continues to increase at a steady rate (Figure 2.4b) which leaves the possibility that the ball would be ejected from the pool with the passing of time. The angular velocity increases and is maintained when the ball reaches the angular velocity of the fluid (sunflower oil). This scenario reflects a reverse of the previous scenario of the bubble in a teacup.

Consider an element (a drop) of the sunflower oil close to the pool wall when the pool is stirred. The element has the same (radial and angular) velocity as the fluid, and of course, equal density as the fluid. And as been suggested in the introduction 1 that a buoyant particle (equal density as the fluid), $R = 2/3$, would act as a fluid tracer immersed in the fluid. The Maxey-Riley equation confirms this as seen in Figure 2.5.

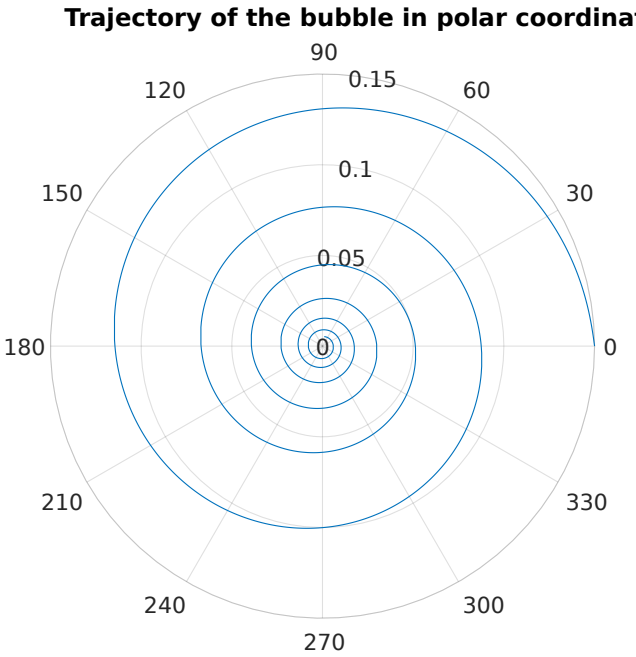

Figure 2.1: The trajectory $(r(t), \theta(t))$ of a bubble (light particle) initially at rest at the edge of the teacup spiraling towards the centre of the stirred tea. For this plot, $A = 2.36$, $R = 1.99$, $\omega_0 = 0.2$, $St = 0.846$, and $Re = 8.56 \times 10^4$.

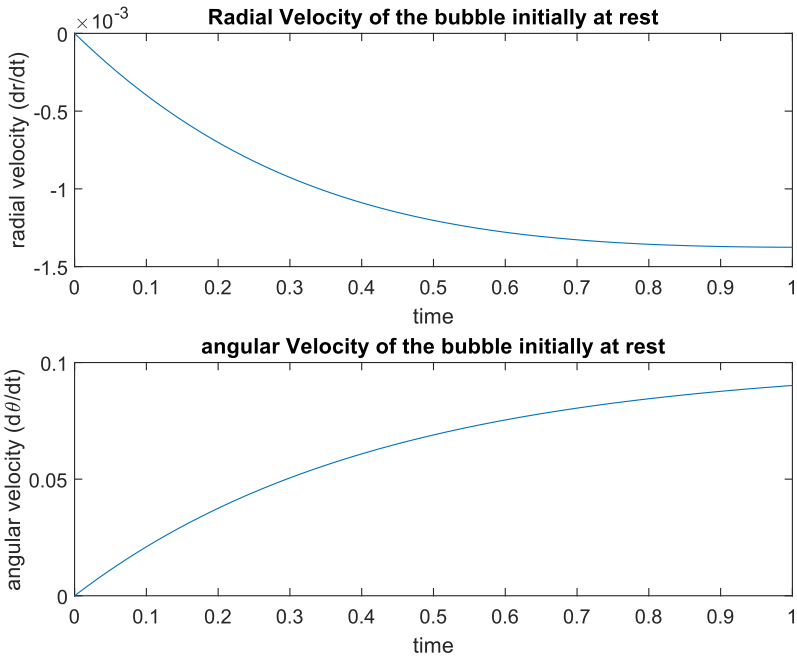

(a) Short term behaviour of the radial and angular velocity of the bubble in Figure 2.1.

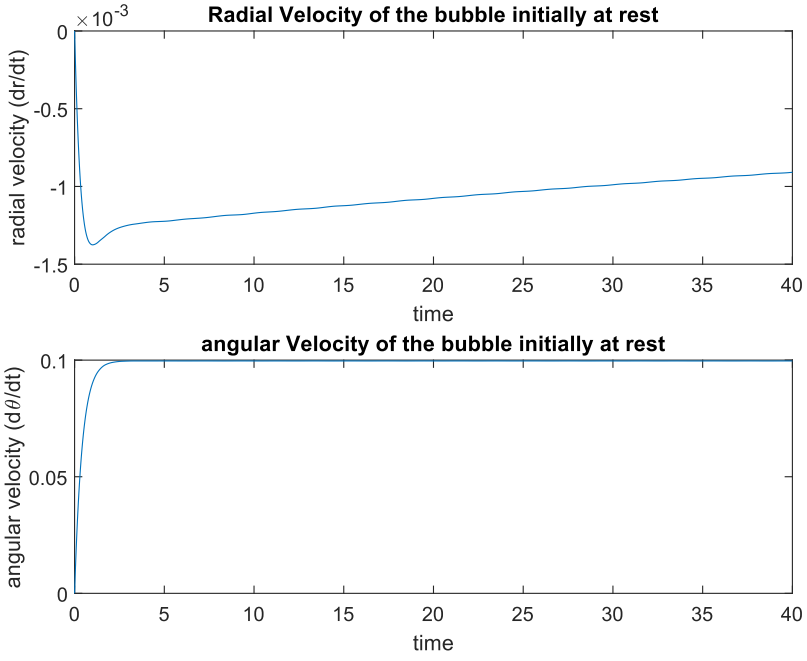

(b) Long term behaviour of the radial and angular velocity of the bubble in Figure 2.1.

Figure 2.2: A plot of the radial and angular velocity of the bubble in Figure 2.1.

The trajectory traced out is perfectly circular, which is expected of a fluid tracer immersed in a fluid with a solid-body vortex velocity flow field.

2.3 Why did the bubble go in?

The explanation why the trajectory takes this shape is anchored on the effects of circular motion, the drag coefficient, and the density ratio of fluid to particle. When the is particle immersed in the rotating fluid and with initial velocity of zero magnitude. It immediately picks up the angular velocity of the fluid and this remains constant all through. The acceleration (deceleration) in the radial direction influences the rate at which the particle spirals inwards (outwards). As previously seen in equation (2.5), the acceleration was given in polar coordinates, the notation is changed below for easier handling.

$$\frac{\mathrm{d}\boldsymbol{v}}{\mathrm{d}t} = \dot{\boldsymbol{v}} = \left(\ddot{r} - r\dot{\theta}^2\right)\hat{e}_r + \left(r\ddot{\theta} + 2\dot{r}\dot{\theta}\right)\hat{e}_\theta \ . \tag{2.9}$$

The radial direction comprises of the linear acceleration ($\ddot{r}$) and the centripetal acceleration ($r\dot{\theta}^2$), while the tangential direction comprise of the linear acceleration ($r\ddot{\theta}$) and the Coriolis acceleration ($2\dot{r}\dot{\theta}$). Since the angular velocity ($\dot{\theta}$) is constant ($\omega_0/2 = 2.5$), the linear acceleration in the tangential direction is zero. This reduces

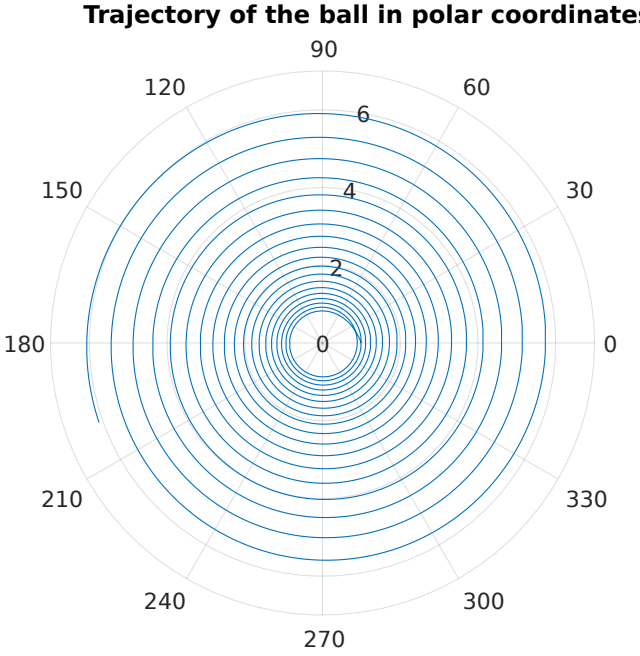

Figure 2.3: The trajectory $(r(t), \theta(t))$ of a ball (heavy particle) initially at rest 1 m from the centre of the pool, spiraling outwards when the pool of sunflower oil is stirred. For this plot, $A = 7.25$, $R = 0.63$, $\omega_0 = 6$, $St = 0.087$, and $Re = 2.71 \times 10^5$.

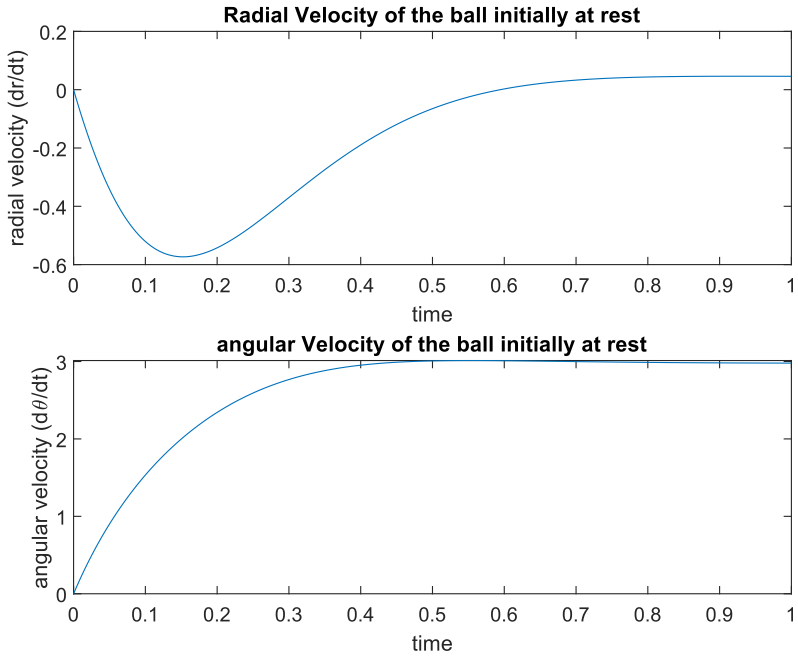

(a) Short term behaviour of the radial and angular velocity of the ball in Figure 2.3.

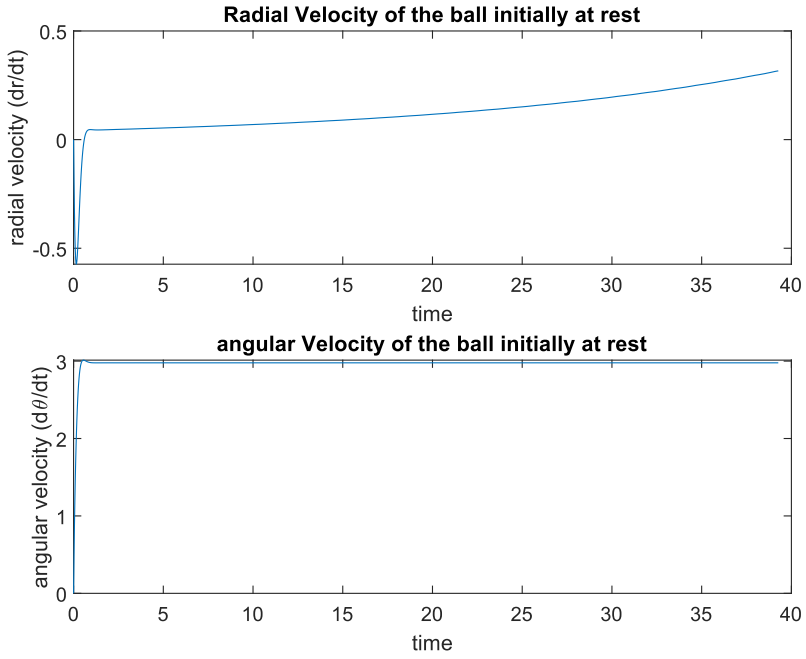

(b) Long term behaviour of the radial and angular velocity of the ball in Figure 2.3.

Figure 2.4: A plot of the radial and angular velocity of the ball in Figure 2.3.

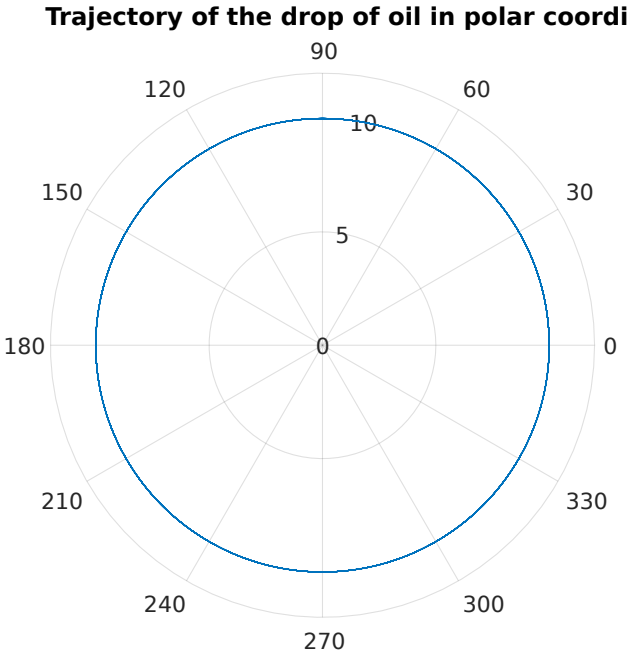

Figure 2.5: The trajectory $(r(t), \theta(t))$ of a drop of sunflower oil (buoyant particle) at the edge of the pool of sunflower oil when it is being stirred. For this plot, $A = 7.25$, $R = 2/3$, $\omega_0 = 6$, $St = 0.087$, and $Re = 2.71 \times 10^5$.

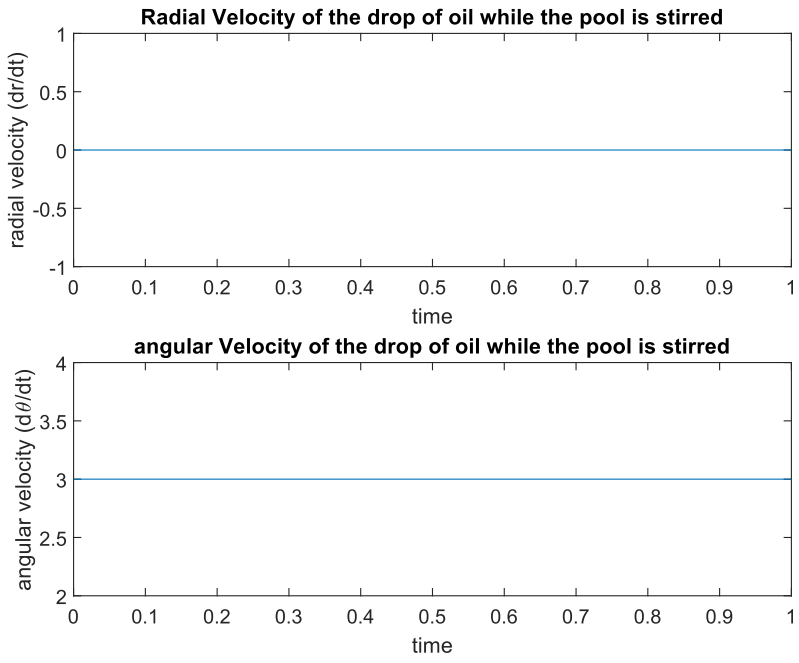

Figure 2.6: A plot of the radial and angular velocity of the drop of sunflower oil in Figure 2.5.

the radial component of the Maxey-Riley equation to the form below

$$\frac{\mathrm{d}^2 r\left(t\right)}{\mathrm{d}t^2} + A\frac{\mathrm{d}r\left(t\right)}{\mathrm{d}t} + \left(\frac{3}{8}R - \frac{1}{4}\right){\omega_0}^2 r\left(t\right) = 0 \ , \tag{2.10}$$

which is a second order ODE whose solution is

$$r\left(t\right) = C_1 \exp\left(\lambda^+ t\right) + C_2 \exp\left(\lambda^- t\right) \tag{2.11}$$

$$\lambda = \ -\frac{A}{2} \ \pm \ \sqrt{\frac{A^2}{4} + \left(1 - \frac{3}{2}R\right){\omega_0}^2} \ . \tag{2.12}$$

The solution above validate that the density ratio of fluid to particle (R) determines the trajectory of the particle. The λ^- is dampened out by the other term in the expression. The solution shows that the radial linear acceleration ($\ddot{r}$) is inversely proportional to the drag coefficient (A). For a light particle, a large drag coefficient—a consequence of low Stokes number—would lead to a slow decrease in the radius of the trajectory and a gradual decrease in the centripetal force ($r\dot{\theta}^2$). The Coriolis acceleration, which influences the tangential acceleration, would slow down as the radial velocity ($\dot{r}$) reduces in magnitude with time. This explains why light particle asymptotically approaches the centre of the vortex. The same science conversely applies for heavy particles.

The cause of the inward (outward) spiral has been anchored to the radial deceleration (acceleration). The cause of the radial acceleration is due to the centrifugal force, which opposes the centripetal force. A heavy particle ($R < 2/3$) is pulled in the direction of the centrifugal force due to its inertia (mass), while a light particle ($R > 2/3$) is pulled away from the centrifugal force. A buoyant particle remains unaffected by the centrifugal force because the effect of the centripetal force cancels this out, and the particle maintains a perfectly circular trajectory. The above scenario is synonymous to the effect of gravity on a body when suspended in the air, the less dense body would go against the gravitational pull, and the denser body would be drawn towards the gravitational pull.

Chapter 3

Finding the particle trajectory in a source-sink pair flow field

A new problem is introduced in this chapter which involves a particle being emitted from the source of a source-sink pair flow field. The question of interest is to find the trajectory of this particle in the fluid. Would the density ratio of fluid to particle make significant changes to the trajectory of the particle as seen to be the case for the solid-body vortex flow field? When the pair is immersed in a constant velocity flow field, what effect would it have on the particle trajectory? If gravity is introduced in the vertical axis, how would this affect the trajectory of the particle? Once again, the Maxey-Riley equation (1.2) would help provide answers to these questions.

3.1 The flow rate and velocity field

A relationship between the flow rate (Q') and velocity of a flow ($\boldsymbol{v}'$) can be derived. For a cylinder with unit height aligned with the source (sink), the source ejects fluid at a rate equal to the rate of fluid flowing out of the cylinder's surface.

The velocity of the fluid flow can be given in polar coordinates as

$$\boldsymbol{v}' = v_r'(r')\,\hat{e}_r\ , \tag{3.1}$$

and the equation for the flow rate is given below as seen in Batchelor[2]

$$\begin{aligned}\int_{\boldsymbol{s}'} \boldsymbol{v}' \cdot \mathbf{d}\boldsymbol{s}' &= v_r'(r').2\pi r' = Q' \\ v_r'(r') &= \frac{Q'}{2\pi r'}\ ,\end{aligned} \tag{3.2}$$

Where $\boldsymbol{s}'$ is the surface over which the fluid spreads, and r' is the radius of the spread. As seen in the above equation, the velocity flow field for the source (sink) has only a radial component, making the tangential component 0.

3.2 Converting to cartesian coordinates

For this current problem, it would be much more useful to have the velocity flow field in cartesian coordinates. This is achieved with the transformation below

$$\begin{bmatrix} \upsilon'_x \\ \upsilon'_y \end{bmatrix} = \begin{bmatrix} \cos\theta' & -\sin\theta' \\ \sin\theta' & \cos\theta' \end{bmatrix} \begin{bmatrix} \upsilon'_r \\ \upsilon'_\theta \end{bmatrix}$$

Which reduces to

$$\begin{aligned} \boldsymbol{\upsilon} &= \left(\frac{Q'\cos\theta'}{2\pi r'}, \frac{Q'\sin\theta'}{2\pi r'} \right) = \left(\frac{Q'x'}{2\pi r'^2}, \frac{Q'y'}{2\pi r'^2} \right) = \left(\frac{Q'x'}{2\pi\left(x'^2+y'^2\right)}, \frac{Q'y'}{2\pi\left(x'^2+y'^2\right)} \right) \\ &= \left(\frac{Q'x'}{2\pi\|\boldsymbol{x'}\|^2}, \frac{Q'y'}{2\pi\|\boldsymbol{x'}\|^2} \right) \end{aligned}$$

Since $r'^2 = x'^2 + y'^2, x' = r'\cos\theta', y' = r'\sin\theta'$
Note that the velocity field above is for a source (sink) located at the origin.

3.3 Velocity field for a source-sink pair

Taking a step further to produce the velocity field for a source-sink pair having different magnitudes—Q'_1 and Q'_2—each placed a distance l' m away from the origin—the source (with Q'_1) located on $(-l', 0)$ and the sink (with Q'_2) on $(l', 0)$. This is achieved by summing the velocity field for both, noting that a sink has a negative flow rate.

$$\upsilon'_x = \frac{Q'_1\left(x'+l'\right)}{2\pi\left(\left(x'+l'\right)^2+y'^2\right)} - \frac{Q'_2\left(x'-l'\right)}{2\pi\left(\left(x'-l'\right)^2+y'^2\right)} \tag{3.3}$$

$$\upsilon'_y = \frac{Q'_1 y'}{2\pi\left(\left(x'+l'\right)^2+y'^2\right)} - \frac{Q'_2 y'}{2\pi\left(\left(x'-l'\right)^2+y'^2\right)}\,. \tag{3.4}$$

Note that this is possible because the distance d from (h, k) to (x, y) satisfies

$$d^2 = (x-h)^2 + (y-k)^2\,. \tag{3.5}$$

To make the problem simpler, the source is moved to the origin and the sink is placed a distance l' m away from the source on the positive x-axis

$$\upsilon'_x = \frac{Q'_1 x'}{2\pi\left(x'^2+y'^2\right)} - \frac{Q'_2\left(x'-l'\right)}{2\pi\left(\left(x'-l'\right)^2+y'^2\right)} \tag{3.6}$$

$$\upsilon'_y = \frac{Q'_1 y'}{2\pi\left(x'^2+y'^2\right)} - \frac{Q'_2 y'}{2\pi\left(\left(x'-l'\right)^2+y'^2\right)}\,. \tag{3.7}$$

3.4 Including the constant flow to the flow field

The velocity field for a constant flow in the x direction is $(V'_\infty, 0)$. Including this in the existing flow results in the new velocity flow field below

$$U'_x = V'_\infty + \frac{Q'_1 x'}{2\pi\left(x'^2 + y'^2\right)} - \frac{Q'_2\left(x' - l'\right)}{2\pi\left(\left(x' - l'\right)^2 + y'^2\right)} \tag{3.8}$$

$$U'_y = \frac{Q'_1 y'}{2\pi\left(x'^2 + y'^2\right)} - \frac{Q'_2 y'}{2\pi\left(\left(x' - l'\right)^2 + y'^2\right)} \, . \tag{3.9}$$

Before this velocity flow field is put to use, a further step is taken to nondimensionalize it with the characteristic length (L') and speed (U') used for the Maxey-Riley equation, although peculiar to the problem of interest. The characteristic length for this problem is chosen as l', the distance between the source and sink. This reduces the expression to

$$u_x = \gamma + \lambda\left[\frac{x}{x^2 + y^2} - \frac{\beta\left(x - 1\right)}{\left(x - 1\right)^2 + y^2}\right] \tag{3.10}$$

$$u_y = \lambda\left[\frac{y}{x^2 + y^2} - \frac{\beta y}{\left(x - 1\right)^2 + y^2}\right] \, , \tag{3.11}$$

where,

$$x = \frac{x'}{L'}, \quad y = \frac{y'}{L'}, \quad \gamma = \frac{V'_\infty}{U'}, \quad \beta = \frac{{Q'}_2}{{Q'}_1} \, , \quad \lambda = \frac{Q_1}{2\pi} \, , \; Q_1 = \frac{{Q'}_1}{L'U'} \, ,$$

and

$$\begin{aligned} \gamma &\equiv \text{nondimensionalized velocity of laminar flow;} \\ \beta &\equiv \text{source-sink strength ratio;} \\ Q_1 &\equiv \text{nondimensionalized flow rate of source; and} \\ \lambda &\equiv \text{scaled valued of nondimensionalized flow rate of source.} \end{aligned}$$

Before now, all parameters in this chapter were considered dimensional parameters. Having nondimensionalized, the nondimensional parameters are without a prime ($'$) floating at their top. It should be noted that every parameter still has the same meaning as before.

3.5 Modifying the Maxey-Riley equation for the source-sink problem

With the velocity flow field in place, the nondimensionalized Maxey-Riley equation is borrowed for use here

$$\frac{\mathrm{d}\boldsymbol{v}}{\mathrm{d}t} - \frac{3}{2}R\frac{\mathrm{D}\boldsymbol{u}}{\mathrm{D}t} = -A\left(\boldsymbol{v} - \boldsymbol{u}\right) + \left(1 - \frac{3}{2}R\right)\boldsymbol{g} \, . \tag{3.12}$$

The parameters in the above equation still have the same meaning as used in the previous chapter. Although the rate of change following the fluid ($\mathrm{D}\boldsymbol{u}/\mathrm{D}t$) is different for this problem. The flow fluid is assumed to be a steady flow, therefore

$$\frac{\partial \boldsymbol{u}}{\partial t} = 0 \ , \tag{3.13}$$

which leaves $\mathrm{D}\boldsymbol{u}/\mathrm{D}t$ defined only by the material derivative

$$\frac{\mathrm{D}\boldsymbol{u}}{\mathrm{D}t} = (\boldsymbol{u} \cdot \boldsymbol{\nabla})\, \boldsymbol{u} \ . \tag{3.14}$$

For the source-sink pair flow field, the material derivative is a complex expression. To take away the trouble of doing the algebra, Maple is employed to obtain this result before importing into MATLAB with the remaining part of the nondimensionalized Maxey-Riley equation and solved numerically using ode solver ode15s [13] (appendix C).

Since the solution of interest is the path (trajectories) $\boldsymbol{X}(t)$ which the particles follow from the source towards the sink, the parameter for the velocity $\boldsymbol{v}(t)$ in the nondimensionalized Maxey-Riley equation (3.12) would would be replaced by the derivatives of $\boldsymbol{X}(t)$

$$\boldsymbol{v}(t) = \frac{\mathrm{d}}{\mathrm{d}t}\boldsymbol{X}(t) \tag{3.15}$$

$$\frac{\mathrm{d}\boldsymbol{v}(t)}{\mathrm{d}t} = \frac{\mathrm{d}^2}{\mathrm{d}t^2}\boldsymbol{X}(t) \ . \tag{3.16}$$

The components of the nondimensionalized Maxey-Riley equation in cartesian coordinates is therefore

$$\frac{\mathrm{d}^2 x}{\mathrm{d}t^2} - \frac{3}{2}RF_x \quad = -A\left(\frac{\mathrm{d}x}{\mathrm{d}t} - u_x\right) + \left(1 - \tfrac{3}{2}R\right) g_x \tag{3.17}$$

$$\frac{\mathrm{d}^2 y}{\mathrm{d}t^2} - \frac{3}{2}RF_y \quad = -A\left(\frac{\mathrm{d}y}{\mathrm{d}t} - u_y\right) + \left(1 - \tfrac{3}{2}R\right) g_y \ , \tag{3.18}$$

where $(\boldsymbol{u} \cdot \boldsymbol{\nabla})\, \boldsymbol{u} = \boldsymbol{F}(x, y) = (F_x, F_y)$, $\boldsymbol{u} = (u_x, u_y)$, $\boldsymbol{g} = (g_x, g_y)$ and $\boldsymbol{X}(t) = (x(t), y(t))$.

3.6 Setup for the initial conditions

The problem is solved for a particle emitted from the source. This phenomenon can be simulated by placing the particle at some distance away from the source and setting the initial velocity equal to the velocity of the flow at that point. To have a wider perspective of the particle trajectory, an ensemble of identical particles is placed on a circle whose centre coincides with the position of the source, so they all have equal distance from the source. So, a step forward is placing the particles at the point where the flow from the source has a velocity of magnitude k. The coordinate of these

points is obtained by solving for the radius of this circle. The radius is obtained by considering a point on the x-axis $(x, 0)$ and solving for the value x when the velocity of the flow from the source has a magnitude of k (a nondimensional parameter). Note that x would then serve as the radius, since this point is exactly a distance x from the source (located at the origin).

$$\left(\frac{\lambda x}{x^2+y^2}\right)^2 + \left(\frac{\lambda y}{x^2+y^2}\right)^2 = k^2 \ . \tag{3.19}$$

Since the point of interest lies on the x-axis, then $y = 0$. This yields

$$x = \frac{\lambda}{k} \ ,$$

and the initial positions become

$$x_0 = r\cos\theta', \quad y_0 = r\sin\theta', \quad r = \frac{\lambda}{k}, \quad 0 \leq \theta' \leq 2\pi \ ,$$

ensuring the particles have an initial velocity of magnitude k.

3.7 Where do the particles go in a source-sink pair flow field?

Considered now is the trajectory for particles in a source-sink flow field with a source flow rate of $1\,\mathrm{m^2 s^{-1}}$ and a sink flow rate of $3\,\mathrm{m^2 s^{-1}}$ placed a distance of $0.65\,\mathrm{m}$ away from the source and with a characteristic velocity of $2.93\,\mathrm{ms^{-1}}$. It should be noted that the effects of gravity and a laminar flow is not considered for this case. The figures below are plots for varying values of R, and with Stokes number of 6.4×10^{-6}.

Investigations reveals that there is no significant change to the trajectory of the particles for either a light, buoyant or heavy particle. It is simply sucked into the sink (red spot) overtime, provided that $Q_2' \geq Q_1'$ $(\beta \geq 1)$. The only exception is the particle that proceeds forward from the sink (blue spot) and continues its trajectory, escaping the pull of the sink. This is because it lies on the stable manifold of the phase plane, and in finite time approaches the stable fixed point (marked $\mathbf{x}$). Ideally, this particle would remain at the fixed point (which is a saddle point), but due to inaccuracies in the numerical computation, it is observed that for light particles (Figure 3.3), it approaches the saddle point and leaves for the sink.

Observation shows that the greater the source-sink strength ratio, the smaller the area covered by the trajectories. Figure 3.4 shows that for unit source-sink strength, the particle trajectory spreads further beyond the area considered. The particle on the stable manifold continues forward in its trajectory, approaching the saddle point at $(-\infty, 0)$.

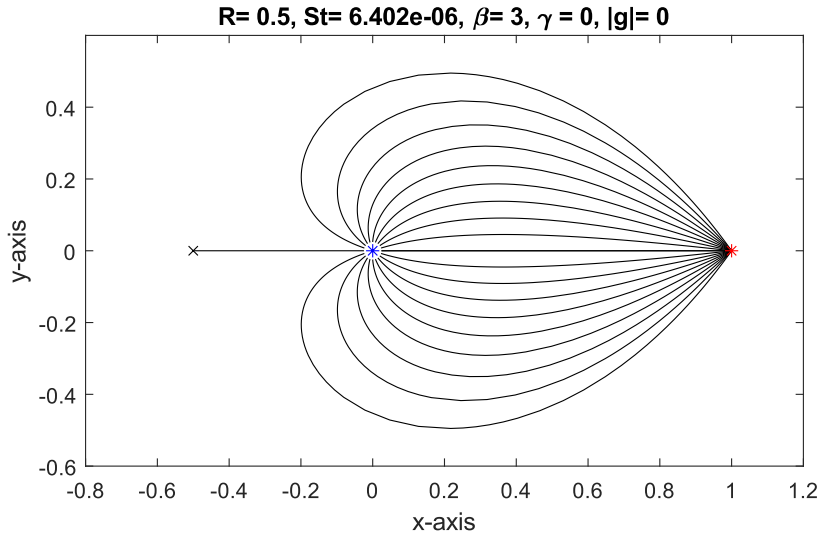

Figure 3.1: The trajectories of particles more dense than the fluid (heavy particles) with a background source-sink pair flow field. For this plot, $R = 0.5$, $St = 6.4 \times 10^{-6}$, $\beta = 3$, $\gamma = 0$, and $|\boldsymbol{g}| = 0$. The blue mark is the source, while the red mark is the sink, and the point marked 'x' is the saddle point.

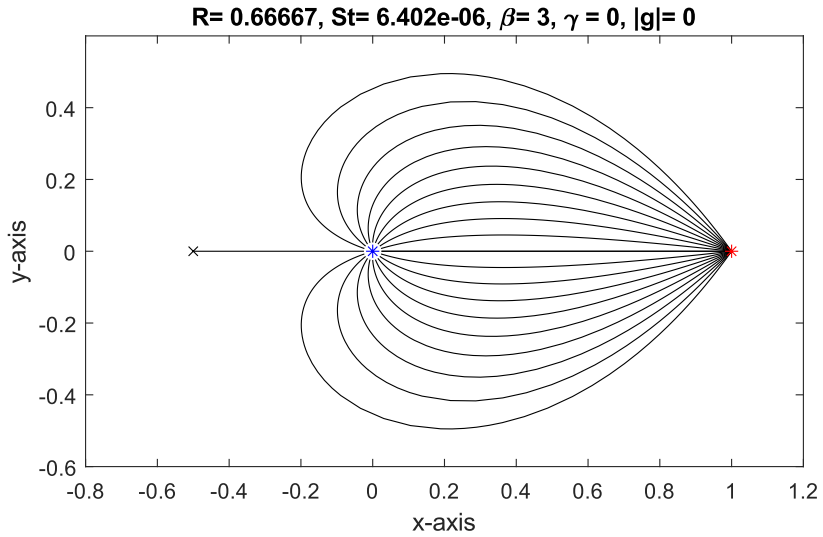

Figure 3.2: The trajectories of particles equally dense as the fluid (buoyant particles) with a background source-sink pair flow field. For this plot, $R = 2/3$, $St = 6.4 \times 10^{-6}$, $\beta = 3$, $\gamma = 0$, and $|\boldsymbol{g}| = 0$. The blue mark is the source, while the red mark is the sink, and the point marked 'x' is the saddle point.

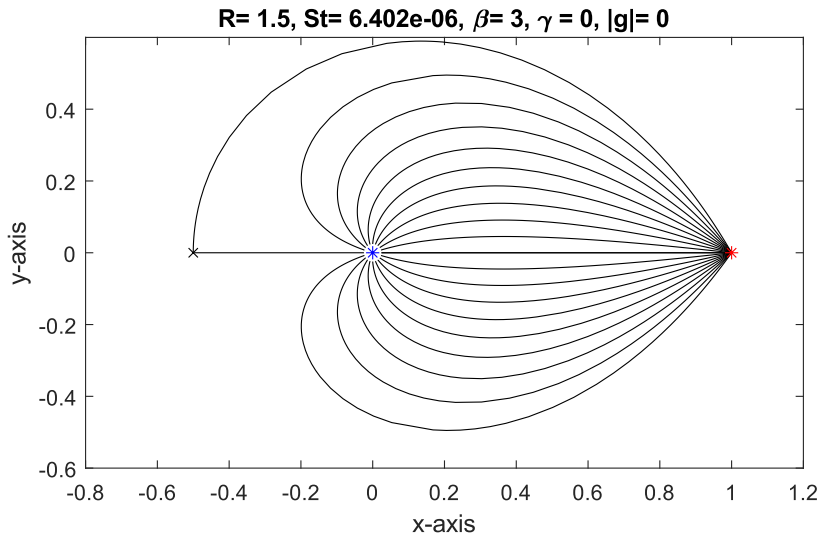

Figure 3.3: The trajectories of particles less dense than the fluid (light particles) with a background source-sink pair flow field. For this plot, $R = 1.5$, $St = 6.4 \times 10^{-6}$, $\beta = 3$, $\gamma = 0$, and $|\boldsymbol{g}| = 0$. The blue mark is the source, while the red mark is the sink, and the point marked 'x' is the saddle point.

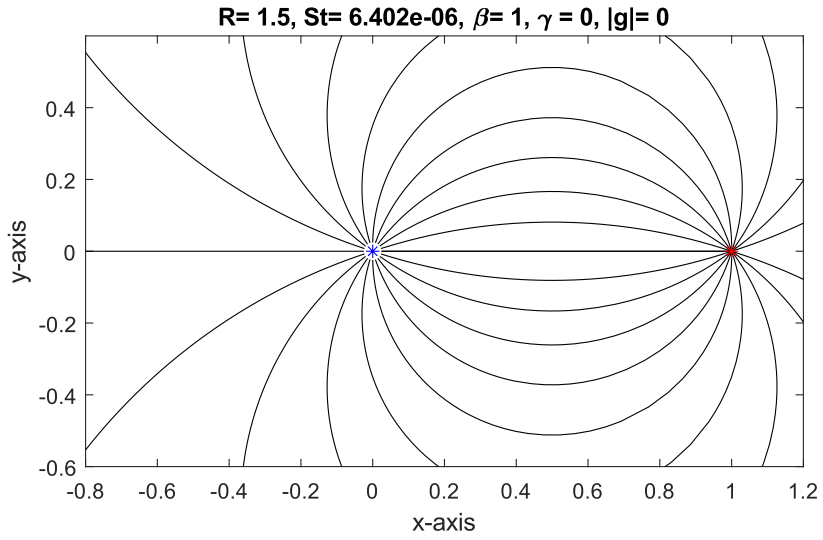

Figure 3.4: The trajectories of particles less dense than the fluid (light particles) with a background source-sink pair flow field. The source and sink are of equal flow rate. For this plot, $R = 1.5$, $St = 6.4 \times 10^{-6}$, $\beta = 1$, $\gamma = 0$, and $|\boldsymbol{g}| = 0$. The blue mark is the source, while the red mark is the sink.

3.8 Effect of gravitational pull on the trajectory of particles

When gravity is introduced in the downward direction, it is observed that the laterally inverted heart-shaped trajectory is skewed in the direction of the gravitational pull for heavy particles ($R < 2/3$), and skewed to the opposite direction of the pull for light particles ($R > 2/3$). And for buoyant particles ($R = 2/3$), the particle is unaffected by the gravitational pull in the vertical direction. This is seen to be the consequence of the coefficient of $\boldsymbol{g}$ in the nondimensionalized Maxey-Riley equation, $(1 - 3R/2)$ (2.2). Numerical investigation reveals that gravitational effect is reduced as the Stokes number gets smaller. Figure 3.5, 3.6 and 3.7 shows the trajectory of heavy, buoyant, and light particles with the same parameters as used in section 3.7, with the introduction of gravity, $g = 10\,\mathrm{ms}^{-2}$.

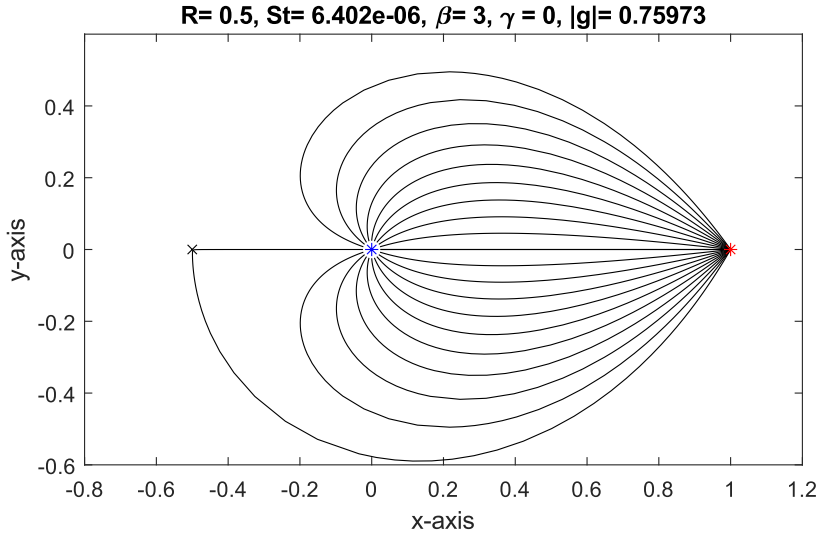

Figure 3.5: The trajectories of particles more dense than the fluid (heavy particles) with a background source-sink pair flow field influenced by gravity. For this plot, $R = 0.5$, $St = 6.4 \times 10^{-6}$, $\beta = 3$, $\gamma = 0$, and $|\boldsymbol{g}| = 0.76$. The blue mark is the source, while the red mark is the sink, and the point marked 'x' is the saddle point.

When a particle is released on the stable manifold of the phase plane, the presence of a gravitational pull takes it off the stable manifold and into the capture region of the sink (Figure 3.5 and 3.7).

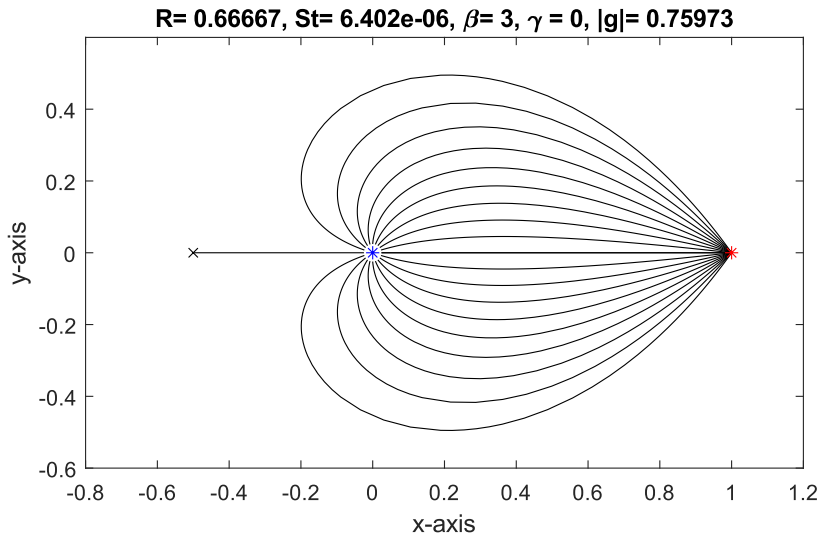

Figure 3.6: The trajectories of particles equally dense as the fluid (buoyant particles) with a background source-sink pair flow field influenced by gravity. For this plot, $R = 2/3$, $St = 6.4 \times 10^{-6}$, $\beta = 3$, $\gamma = 0$, and $|\boldsymbol{g}| = 0.76$. The blue mark is the source, while the red mark is the sink, and the point marked 'x' is the saddle point.

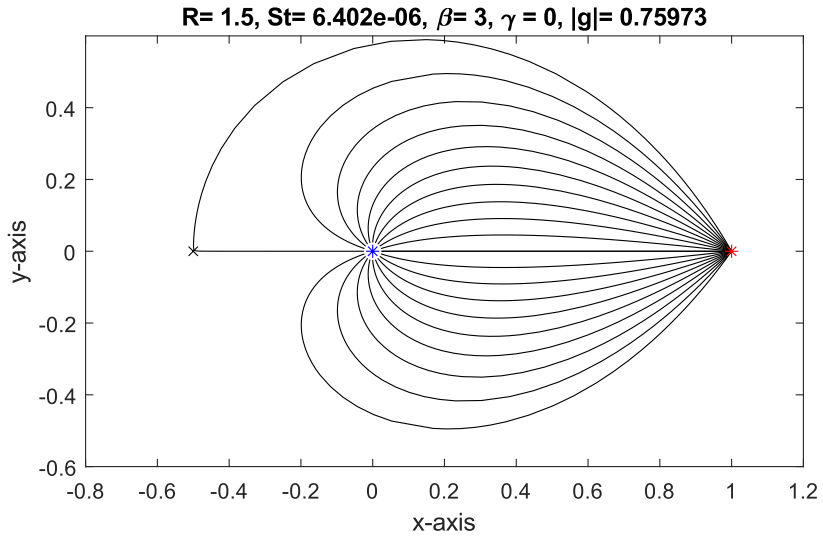

Figure 3.7: The trajectories of particles less dense than the fluid (light particles) with a background source-sink pair flow field influenced by gravity. For this plot, $R = 1.5$, $St = 6.4 \times 10^{-6}$, $\beta = 3$, $\gamma = 0$, and $|\boldsymbol{g}| = 0.76$. The blue mark is the source, while the red mark is the sink, and the point marked 'x' is the saddle point.

3.9 Effect of laminar flow on the trajectory of particles

Now the constant flow is introduced into the field (without gravity). With other parameters unchanged and $V'_\infty = 2\,\mathrm{ms}^{-1}$, all particles—except that on the stable manifold—are observed to flow directly into the sink provided $\beta \geq 1$ for $V'_\infty \geq 1\,\mathrm{ms}^{-1}$. Figure 3.9 and 3.10 shows the particle on the stable manifold leave for the sink, this is a result of numerical inaccuracies. Ideally, the particle would approach the fixed point in finite time and remain there. The laminar flow reduces the area covered by the particle trajectory, so with increased laminar flow speed, the smaller the spread. Observations show that the effect of laminar flow improves as the Stokes number increases, and this applies for all values of R. Note that these observations are true when the laminar flow is towards the sink (positive x-axis).

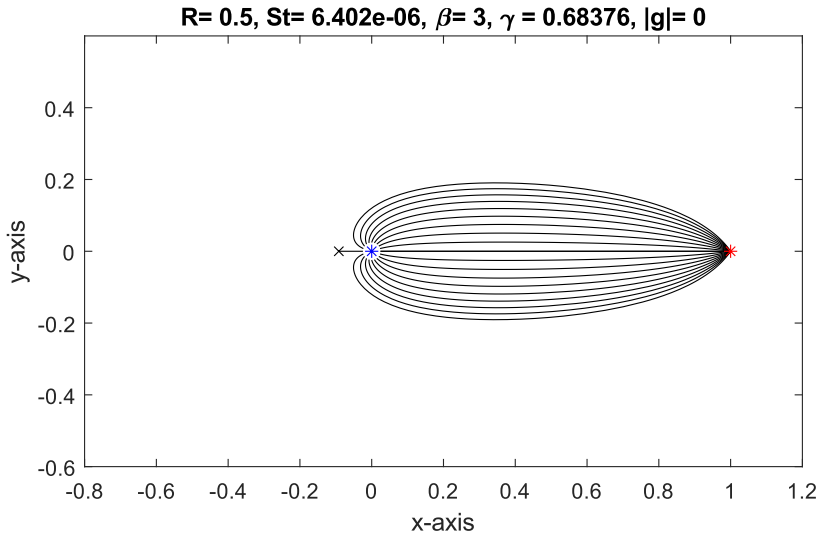

Figure 3.8: The trajectories of particles more dense than the fluid (heavy particles) with a background source-sink pair flow field influenced by a laminar flow. For this plot, $R = 0.5$, $St = 6.4 \times 10^{-6}$, $\beta = 3$, $\gamma = 0.68$, and $|\boldsymbol{g}| = 0$. The blue mark is the source, while the red mark is the sink, and the point marked 'x' is the saddle point.

When the flow is in the opposite direction, it pushes the particles away from the sink in the direction of the flow. For this scenario, the source-sink strength ratio (β) required to pull all the particles into the sink would be far greater than previous cases, and the fixed point would be displaced from the existing location. For $V'_\infty = -1\,\mathrm{ms}^{-1}$ and $\beta = 3$, only few particles were pulled into the sink (Figure 3.11)—less than 20%. It took a source-sink strength ratio of at least 9.2 to counteract the effect of the opposing laminar flow, thereby pulling all particles into the sink.

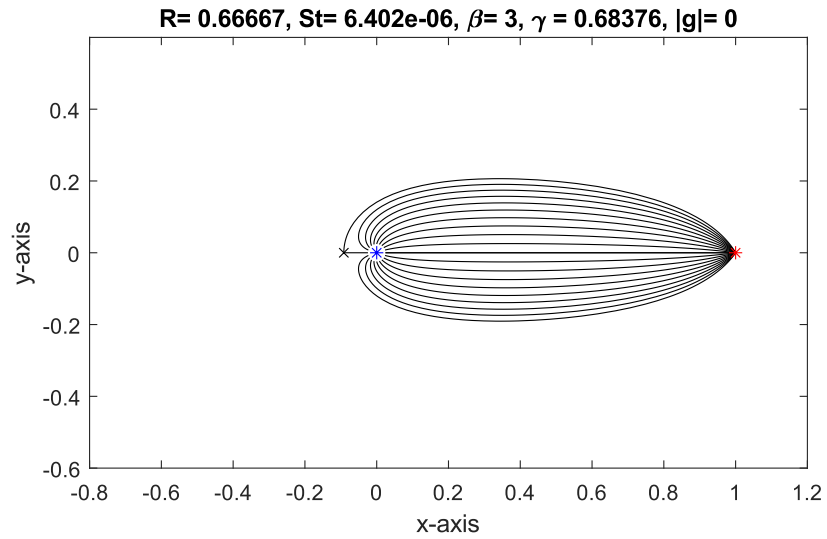

Figure 3.9: The trajectories of particles equally dense as the fluid (buoyant particles) with a background source-sink pair flow field influenced by a laminar flow. For this plot, $R = 2/3$, $St = 6.4 \times 10^{-6}$, $\beta = 3$, $\gamma = 0.68$, and $|\boldsymbol{g}| = 0$. The blue mark is the source, while the red mark is the sink, and the point marked 'x' is the saddle point.

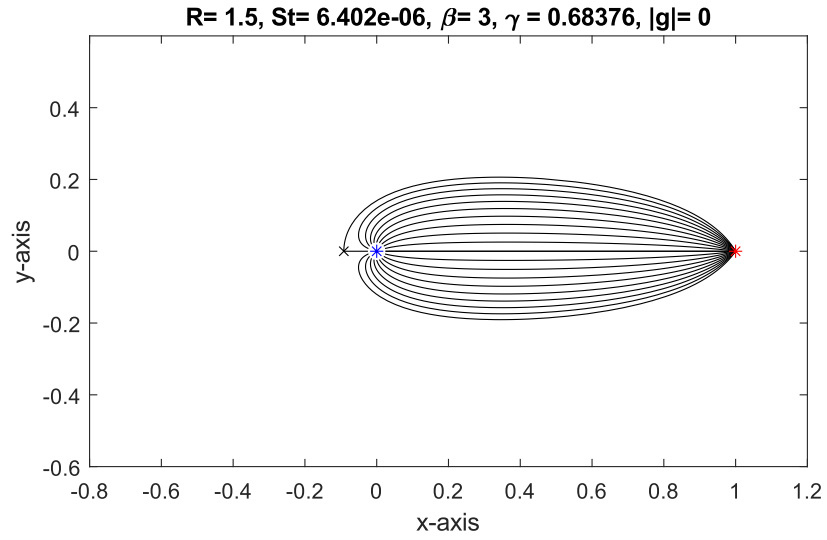

Figure 3.10: The trajectories of particles less dense than the fluid (light particles) with a background source-sink pair flow field influenced by a laminar flow. For this plot, $R = 1.5$, $St = 6.4 \times 10^{-6}$, $\beta = 3$, $\gamma = 0.68$, and $|\boldsymbol{g}| = 0$. The blue mark is the source, while the red mark is the sink, and the point marked 'x' is the saddle point.

3.10 Mathematical model for extracting aerosol particles from a sick patient

Now equipped with the knowledge of the particle trajectory for varying scenarios, the derived flow field with the Maxey-Riley equation would be used to design a mathematical model for an aerosol extractor.

Humans emit aerosol particles of varying sizes while breathing or sneezing/coughing [5, 24]. For a sick patient, these aerosols would have viruses trapped in them [11]. So, the goal is to design a model that can trap these aerosols as they are emitted. Now consider a patient who emits aerosol particles of an average diameter of $20\mu\,\mathrm{m}$ [5] at an average speed of $2.93\,\mathrm{ms}^{-1}$ [5, 24]–this value would be taken as the characteristic speed. The aerosol particles are water droplets, so would have a density of $1000\,\mathrm{kg/m}^3$ at room temperature (25°C), with the air density about $1.184\,\mathrm{kg/m}^3$ [27]. The flow rate of the patient's breath is observed to be $1\,\mathrm{m}^2\mathrm{s}^{-1}$. The kinematic viscosity of air at 25°C is given as $1.56 \times 10^{-5}\,\mathrm{m}^2\mathrm{s}^{-1}$ [27].

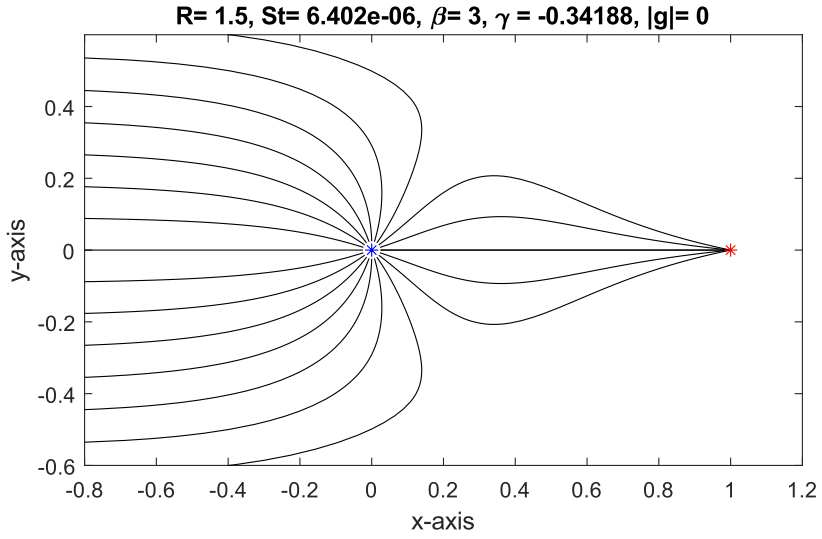

Figure 3.11: The trajectories of particles less dense than the fluid (light particles) with a background source-sink pair flow field opposed by a laminar flow. For this plot, $R = 1.5$, $St = 6.4 \times 10^{-6}$, $\beta = 3$, $\gamma = -0.34$, and $|\boldsymbol{g}| = 0$. The blue mark is the source, while the red mark is the sink.

In addition to the above measurements, the patient is placed in a room with an air duct on the wall behind the patient's head, who lies still on the bed. The air duct is a low velocity duct with an average velocity of $2.5\,\mathrm{ms}^{-1}$, which would serve as the laminar flow. The average distance the aerosol particles cover when emitted is $0.65\,\mathrm{m}$ [5, 24]–this would be taken as the characteristic length. So the extractor would be

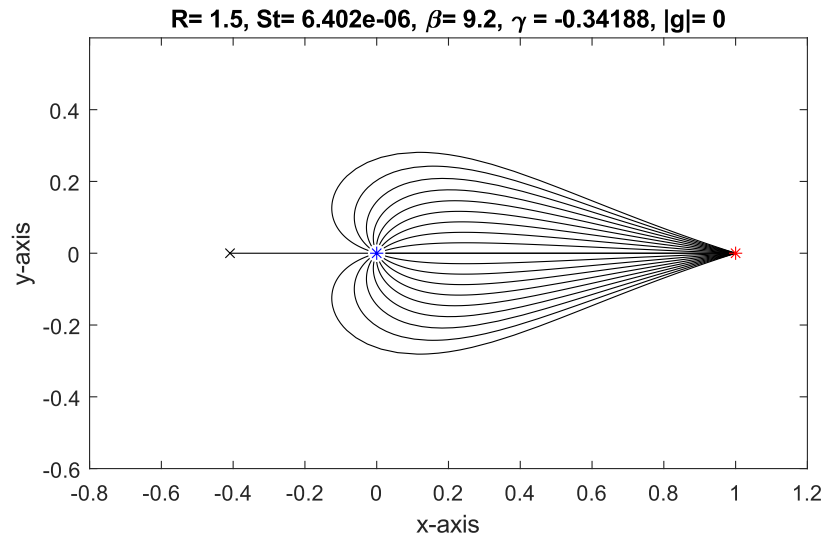

Figure 3.12: The trajectories of particles less dense than the fluid (light particles) with a background source-sink pair flow field opposed by a laminar flow, but captured into the sink. For this plot, $R = 1.5$, $St = 6.4 \times 10^{-6}$, $\beta = 9.2$, $\gamma = -0.34$, and $|\boldsymbol{g}| = 0$. The blue mark is the source, while the red mark is the sink, and the point marked 'x' is the saddle point.

placed at this distance towards the feet of the patient, about the same horizon as the patient's head. All these happens under the influence of gravity at $10\,\mathrm{ms}^{-2}$. Since the air flow in the room is in the direction of the aerosol extractor, the extractor can be set to at least $3\,\mathrm{m}^2\mathrm{s}^{-1}$ which would successfully capture all the aerosols emitted from the patient, and this would equally reduce the area of the spread before complete capture. The trajectory of the aerosols is seen in Figure 3.13.

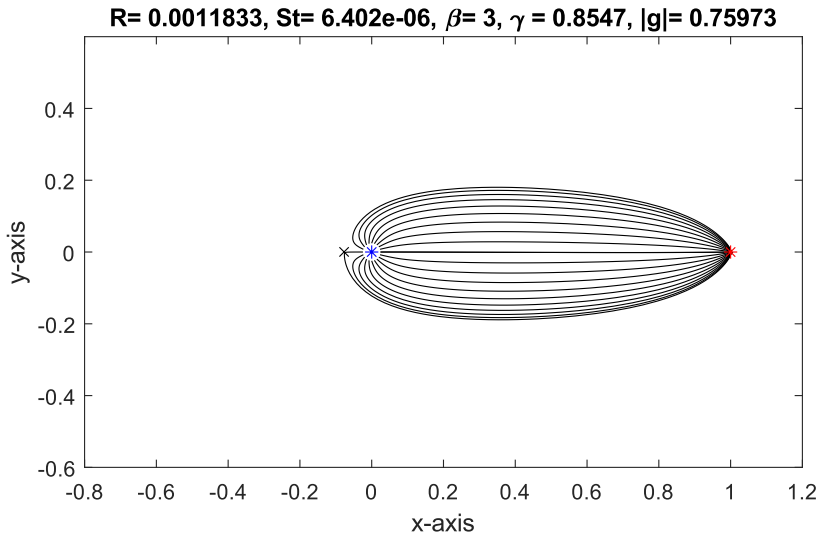

Figure 3.13: The trajectories of aerosols from a breathing patient being captured by an aerosol extractor. The flow is influenced by gravity and a laminar flow which is in the direction of the sink. For this plot, $R = 1.18 \times 10^{-3}$, $St = 6.4 \times 10^{-6}$, $\beta = 3$, $\gamma = 0.85$, and $|\boldsymbol{g}| = 0.76$. The blue mark is the patient's nostril (source), while the red mark is the aerosol extractor (sink), and the point marked 'x' is the saddle point.

With the other parameters fixed, if the air duct is placed on the opposite end of the room, a distance away from the feet of the patient. Figure 3.14 reveals that the source-sink strength ratio would be about 6 times ($\beta = 18$) the amount needed when the laminar flow was towards the extractor.

The results are not surprising as it appears to be the combined effect of gravity and a laminar flow on a heavy particle as seen in previous sections. And the particle on the stable manifold is swept into the capture region by gravity as expected.

An extractor can be designed based on the above model, it can be adapted for use in hospitals to trap the aerosols from COVID-19 patients when operated upon by the doctors, and for patients who have to be admitted due to severity of their medical condition.

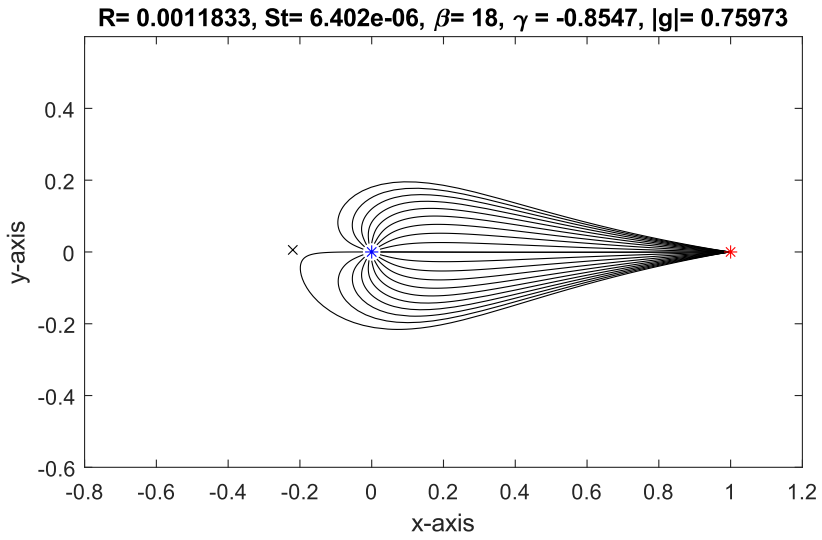

Figure 3.14: The trajectories of aerosols from a breathing patient being captured by an aerosol extractor. The flow is influenced by gravity and a laminar flow which pushes the aerosols away from the sink. For this plot, $R = 1.18 \times 10^{-3}$, $St = 6.4 \times 10^{-6}$, $\beta = 18$, $\gamma = -0.85$, and $|\boldsymbol{g}| = 0.76$. The blue mark is the patient's nostril (source), while the red mark is the aerosol extractor (sink), and the point marked 'x' is the saddle point.

Chapter 4

Conclusion

Going through the previous pages has led to several findings which would be summarized in this chapter. Chapter one introduced the problem of particle motion in a fluid for the solid-body vortex and the source-sink pair flow field. And the question asked was what the trajectory of the particle would be for both flow fields when we consider particles that are equally dense (buoyant) as the fluid, less dense (light) than the fluid, and more dense (heavy) than the fluid. For this question, the Maxey-Riley equation was introduced, which is a rework of Tchen 1947 PhD thesis [25] due to the many errors contained in his result.

Using the Maxey-Riley equation required the neglect of the Basset's history term, as this makes the equation much more difficult to solve due to the nonlocality the integral operator introduces [17]. The benefit of this neglect is that the equation reduces to an ordinary differential equation which can be easily solved with various numerical techniques, or by employing software to increase speed. The consequence of this neglect has been pointed out to change the nature of the solution from an algebraic asymptotic decay to an exponential convergence [12]. But under given conditions, the effect of the history term is negligible and can be ignore [17].

The Maxey-Riley equation was nondimensionalized and converted to polar coordinates to make it suitable for analysis. This was because the trajectory path for a particle in a solid-body vortex would be circular, and polar coordinates are helpful in accounting for the forces that influence the motion of the particle. The question of the trajectory of a light particle in a solid-body vortex was reposed as: where would the bubbles in a teacup move to when stirred? The solution of the Maxey-Riley equation for the solid-body vortex revealed that a light particle (bubble) will spiral inward, approaching the vortex core asymptotically (Figure 2.1). While a solid particle would spiral outward and may be ejected from the fluid (Figure 2.3). A buoyant particle would follow a perfectly circular trajectory, acting as a fluid tracer immersed in the fluid (Figure 2.5). The cause for these phenomena is anchored to the increase/decrease in the radial acceleration which is caused by the centrifugal force pulling the heavy particle outward, and the greater centripetal force that pulled the light particle inwards. The

effect of the centripetal and centrifugal force cancels out for a buoyant particle, which causes the particle to follow the fluid.

For the source-sink problem, the Maxey-Riley equation was solved in cartesian coordinates. The expression for the velocity field was derived in polar coordinates, in terms of the flow rate. The tangential component of the derived velocity field was 0, while the radial component was defined in terms of the flow rate and radius. Since the source-sink problem is considered in cartesian coordinate, the velocity field was transformed to cartesian coordinates. The source is located on the origin, and the sink was placed a distance l' m from the origin on the x-axis. The solution to the Maxey-Riley equation was sought for an ensemble of particles having equal distance from the source with an initial velocity equal to the velocity of the flow from the source at their current position.

The solution for the Maxey-Riley equation reveals that for all values of R, the particles emitted from the source would flow into the sink provided $\beta \geq 1$, in the absence of gravity and laminar flow. But the particle emitted on the stable manifold would continue forward in its trajectory and approach the fixed (saddle) point in finite time. Investigation showed that the greater the source-sink strength ratio (β), the smaller the area covered by the particle trajectory.

It was observed that under the influence of gravity, the trajectories of buoyant particles are unaffected and maintains the same shape as when gravity is absent. This is a consequence of the coefficient of $\boldsymbol{g}$ in the nondimensionalized Maxey-Riley equation (2.2), as $R = 2/3$ makes the coefficient zero. For a heavy particle, the trajectory is skewed in the direction of the gravitational pull, while a light particle is skewed in the opposite direction. And the smaller the Stokes number, the lesser the influence of gravity on the particle trajectory. The phenomenon of light particles moving away from the pull of gravity is also seen in aerosols that are less dense than air in a room. When an individual sneezes and emits droplets (aerosols), the heavy droplets fall to the ground and the tiny ones, which are less dense than air, would remain afloat in the room [11]. The simulation in this work does not show this particular effect, since the presence of a sink pulls the aerosols in before they have a chance to spread. But Figure 3.5 and 3.7 reveals this as the particle on the stable manifold leaves for the sink in the direction that gravity influences for a light or heavy particle.

The effect of a laminar flow in a source-sink pair flow field is advantageous. When the flow is in the direction of the sink, it drives all particles to the sink easily. And the effect is increased as the Stokes number reduces for all values of R. When the constant flow is in the opposite direction from the sink, it pushes the particles in the direction of the flow, and the sink requires an amplified strength to counteract this effect and suck the particles in. For $V'_\infty = -1\,\mathrm{ms}^{-1}$, $\beta \geq 9.2$ for the sink to suck in all particles. Having gravity and constant flow present with the source-sink pair flow field comes with no surprises. The trajectory of the particle is influenced by the combined effect of both events.

A mathematical model was presented for an aerosol extractor. The extractor is designed to trap aerosol particles from a sick patient, whose aerosols would contain a virus [11], for example COVID-19. The right measurements were considered for the

aerosol and air density, speed, and the velocity of the laminar air flow in the room. The result showed that an extractor would require a strength of at least $3\,\mathrm{m^2 s^{-1}}$ to trap all the aerosols emitted by the sick patient in a room with an air duct whose velocity is $2.5\,\mathrm{ms^{-1}}$ in the direction of the sink. When the laminar flow is moving away from the sink, the extractor would require a strength of at least $18\,\mathrm{m^2 s^{-1}}$ to trap all the aerosols released. This design is a setup for a 2D space, which limits its direct application without having to extend the results to a 3D space (which we live in).

A future possibility for this research asides extending the results to a 3 dimensional space for both flow fields, is to consider zooplanktons that have the same density as microplastic, and use the Maxey-Riley equation to model the proportion of microplastics that would be consumed by their predators, for example *Aurelia aurita* (Jelly fish). This would help predict how our activities as humans would affect aquatic life in the coming years, considering our increasing level of water pollution with nonbiodegradables.

Appendix A

Nondimensionalizing the Maxey-Riley equation

This section is concerned with the algebra that reduced the Maxey-Riley equation into the form as seen in (2.2).

$$m_p' \frac{\mathrm{d}\boldsymbol{V'}}{\mathrm{d}\tau'} = m_f' \frac{\mathrm{D}\boldsymbol{U'}}{\mathrm{D}\tau'} + \left(m_p' - m_f'\right)\boldsymbol{g}' + \ 6\pi a'\mu' \left[\boldsymbol{U'} - \boldsymbol{V'} + \frac{a'^2}{6}\Delta\boldsymbol{U'}\right]$$
$$- \frac{m_f'}{2}\left[\frac{\mathrm{d}\boldsymbol{V'}}{\mathrm{d}\tau'} - \frac{\mathrm{D}}{\mathrm{D}\tau'}\left(\boldsymbol{U'} + \frac{a'^2}{10}\Delta\boldsymbol{U'}\right)\right] + \int_0^{\tau'} \frac{1}{\sqrt{\tau' - s'}} \frac{\mathrm{d}}{\mathrm{d}s'}\left[\boldsymbol{U'} - \boldsymbol{V'} + \frac{a'^2}{6}\Delta\boldsymbol{U'}\right] \mathrm{d}s' \ .$$

For the solid-body vortex and source-sink pair flow fields, $\Delta\boldsymbol{U'} = 0$, and for simplification, the Basset's history term is neglected. This reduces the equation to

$$m_p' \frac{\mathrm{d}\boldsymbol{V'}}{\mathrm{d}\tau'} = m_f' \frac{\mathrm{D}\boldsymbol{U'}}{\mathrm{D}\tau'} + \left(m_p' - m_f'\right)\boldsymbol{g}' + \ 6\pi a'\mu' \left[\boldsymbol{U'} - \boldsymbol{V'}\right] - \frac{m_f'}{2}\left[\frac{\mathrm{d}\boldsymbol{V'}}{\mathrm{d}\tau'} - \frac{\mathrm{D}\boldsymbol{U'}}{\mathrm{D}\tau'}\right]$$
$$\left(m_p' + \frac{m_f'}{2}\right)\frac{\mathrm{d}\boldsymbol{V'}}{\mathrm{d}\tau'} = \left(m_p' + \frac{m_f'}{2}\right)\frac{\mathrm{D}\boldsymbol{U'}}{\mathrm{D}\tau'} + \left(m_p' - m_f'\right)\boldsymbol{g}' + \ 6\pi a'\mu' \left[\boldsymbol{U'} - \boldsymbol{V'}\right]$$
$$\left(\frac{m_f' + 2m_p}{2}\right)\frac{\mathrm{d}\boldsymbol{V'}}{\mathrm{d}\tau'} = \frac{3}{2}m_f' \frac{\mathrm{D}\boldsymbol{U'}}{\mathrm{D}\tau'} + \left(m_p' - m_f'\right)\boldsymbol{g}' + \ 6\pi a'\mu' \left[\boldsymbol{U'} - \boldsymbol{V'}\right]$$
$$\frac{\mathrm{d}\boldsymbol{V'}}{\mathrm{d}\tau'} = \frac{3}{2}\left(\frac{2m_f'}{m_f' + 2m_p'}\right)\frac{\mathrm{D}\boldsymbol{U'}}{\mathrm{D}\tau'} + \left(\frac{2m_f' - 2m_p'}{m_f' + 2m_p'}\right)\boldsymbol{g}' + \frac{12\pi a'\mu'}{m_f' + 2m_p'}\left[\boldsymbol{U'} - \boldsymbol{V'}\right] \ .$$

Set

$$R = \frac{2m_f'}{m_f' + 2m_p'} \times \frac{\frac{1}{\frac{4}{3}\pi a'^3}}{\frac{1}{\frac{4}{3}\pi a'^3}} = \frac{2\rho_f'}{\rho_f' + 2\rho_p'} \ ,$$

where $\frac{4}{3}\pi a'^3$ is the volume of the spherical particle, ρ_f' is the fluid density and ρ_p' is the particle density. Therefore,

$$\frac{2m_f' - 2m_p'}{m_f' + 2m_p'} = 1 - \frac{3}{2}R \ ,$$

and

$$\frac{12\pi a'\mu'}{m'_f+2m'_p}=\frac{6\pi a'\mu' R}{m'_f}\ =\frac{6\pi a'\mu' R}{\frac{4}{3}\pi a'^3\rho'_f}=\frac{9}{2}\pi\upsilon R=\frac{R}{\frac{2}{9}\left(\frac{a'}{L'}\right)^2\frac{U'L'}{\nu'}\cdot\frac{L'}{U'}}=\frac{R}{\frac{2}{9}\left(\frac{a'}{L'}\right)^2 Re\frac{L'}{U'}}\ ,$$

where $\nu'=\frac{\mu'}{\rho'_f}$ is the kinematic viscosity, L' is the characteristic length, U' is the characteristic speed and $Re=\frac{U'L'}{\nu'}$ is the Reynolds number. Now set

$$St=\frac{2}{9}\left(\frac{a'}{L'}\right)^2 Re\ ,$$

then our previous result further simplifies to

$$\frac{R}{\frac{2}{9}\left(\frac{a'}{L'}\right)^2 Re\frac{L'}{U'}}=\frac{R}{St}\cdot\frac{U'}{L'}=A\frac{U'}{L'}\ ,$$

where

$$A=\frac{R}{St}\ .$$

This reduces the equation to

$$\frac{\mathrm{d}\boldsymbol{V'}}{\mathrm{d}\tau'}=\frac{3}{2}R\frac{\mathrm{D}\boldsymbol{U'}}{\mathrm{D}\tau'}+\left(1-\frac{3}{2}R\right)\boldsymbol{g'}+A\frac{U'}{L'}\left[\boldsymbol{U'}-\boldsymbol{V'}\right]\ .$$

Proceeding to nondimensionalize, take

$$\boldsymbol{\upsilon}=\frac{\boldsymbol{V'}}{\langle\boldsymbol{V'}\rangle},\quad \boldsymbol{u}=\frac{\boldsymbol{U'}}{\langle\boldsymbol{U'}\rangle},\quad t=\frac{\tau'}{\langle\tau'\rangle},\quad \boldsymbol{g}=\frac{\boldsymbol{g'}}{\langle\boldsymbol{g'}\rangle}\ .$$

Where, $\boldsymbol{\upsilon},\boldsymbol{u},t$ and $\boldsymbol{g}$ are dimensionless parameters of their corresponding dimensional parameters, and $\langle\boldsymbol{V'}\rangle,\langle\boldsymbol{U'}\rangle,\langle\boldsymbol{g'}\rangle$ and $\langle\tau'\rangle$ are scaling parameters.

$$\frac{\mathrm{d}\boldsymbol{\upsilon}}{\mathrm{d}t}\frac{\langle\boldsymbol{V'}\rangle}{\langle\tau'\rangle}=\frac{3}{2}R\frac{\mathrm{D}\boldsymbol{u}}{\mathrm{D}\tau'}\frac{\langle\boldsymbol{U'}\rangle}{\langle\tau'\rangle}+\left(1-\frac{3}{2}R\right)\langle\boldsymbol{g'}\rangle\,\boldsymbol{g}+A\frac{U'}{L'}\left[\boldsymbol{u}\,\langle\boldsymbol{U'}\rangle-\boldsymbol{\upsilon}\,\langle\boldsymbol{V'}\rangle\right]$$

$$\frac{\mathrm{d}\boldsymbol{\upsilon}}{\mathrm{d}t}=\frac{3}{2}R\frac{\langle\boldsymbol{U'}\rangle}{\langle\boldsymbol{V'}\rangle}\frac{\mathrm{D}\boldsymbol{u}}{\mathrm{D}\tau'}+\left(1-\frac{3}{2}R\right)\frac{\langle\tau'\rangle}{\langle\boldsymbol{V'}\rangle}\langle\boldsymbol{g'}\rangle\,\boldsymbol{g}+A\frac{U'}{L'}\langle\tau'\rangle\left[\boldsymbol{u}\frac{\langle\boldsymbol{U'}\rangle}{\langle\boldsymbol{V'}\rangle}-\boldsymbol{\upsilon}\right]\ .$$

Let

$$\frac{\langle\boldsymbol{U'}\rangle}{\langle\boldsymbol{V'}\rangle}=1\implies\quad\langle\boldsymbol{U'}\rangle=\langle\boldsymbol{V'}\rangle=U'$$

$$\frac{U'}{L'}\langle\tau'\rangle=1\implies\quad\langle\tau'\rangle=\frac{L'}{U'}\ ,$$

and

$$\frac{\langle\tau'\rangle}{\langle\boldsymbol{V'}\rangle}\langle\boldsymbol{g'}\rangle=1\Longrightarrow\langle\boldsymbol{g'}\rangle=\frac{U'^2}{L'}\ .$$

Therefore,

$$\frac{\mathrm{d}\boldsymbol{\upsilon}}{\mathrm{d}t}=\frac{3}{2}R\frac{\mathrm{D}\boldsymbol{u}}{\mathrm{D}t}+\left(1-\frac{3}{2}R\right)\boldsymbol{g}+A\left[\boldsymbol{u}-\boldsymbol{\upsilon}\right]\ ,\tag{A.1}$$

and

$$\boldsymbol{\upsilon}=\frac{\boldsymbol{V'}}{U'},\quad \boldsymbol{u}=\frac{\boldsymbol{U'}}{U'},\quad t=\frac{\tau'U'}{L'},\quad \boldsymbol{g}=\frac{\boldsymbol{g'}L'}{U'^2}\ .\tag{A.2}$$

Appendix B

MATLAB code for the solution to the Maxey-Riley equation using solid-body vortex flow field

```
%This script solves the given ODE for the components of the Maxey-Riley eq
%The result of this is the position
%Script name: Maxey_Riley_solver_position_polar
%Author: Ajayi Olayinka Josiah

char_omega= pi;%Characteristic angular velocity
L= 15e-2;%m Characteristic length
U= char_omega*L/2;%Characteristic linear velocity
time= [0:.01:250]*U/L;
v0= [L,0,0,0]';%Intial position and velocity
rho_f= 971.82;%kg/m3 : fluid density at room temperature
rho_p= 1.4;%kg/m3 : particle density at room temperature
a= 1e-3;%m : radius of particle
nu= 4.13e-7;%m2/s : kinematic viscosity
R= 2*rho_f/(rho_f + 2*rho_p);%When R= 2/3,<2/3 or >2/3, the
%particle is buoyant, heavy or light respectively
Re= U*L/nu;%Reynolds number
St= (2/9)*(a/L)^2*Re;%Stokes number
A= R/St;%Stokes drag
omega0= (0.2*pi)/char_omega;%angular velocity

%This is the solution to the Maxey-Riley equation
[t,v]= ode23(@(t,v) maxeyODE_position_r(t,v,A,R,omega0),time,v0);

figure(1)
polarplot(v(:,3),v(:,1))
title('Trajectory of the bubble in polar coordinates')

figure(2)
subplot(2,1,1)
plot(t,v(:,2))
xlim([0 1])
xlabel('time')
```

```
ylabel('radial velocity (dr/dt)')
title('Radial Velocity of the bubble initially at rest')

subplot(2,1,2)
axis tight
plot(t,v(:,4))
xlim([0 1])
xlabel('time')
ylabel('angular velocity (d\theta/dt)')
title('angular Velocity of the bubble initially at rest')


function dy_dx = maxeyODE_position_r(t,v,A,R,omega0)
%This function houses the set of ODE for the x/y-components of the
%Maxey-Riley equation in polar form
%   This would be called in the script that solves it


dy_dx(1,1) = v(2);
dy_dx(2,1) = -(3/8)*R*omega0^2*v(1) - A*v(2) + v(1)*(v(4))^2;
dy_dx(3,1) = v(4);
dy_dx(4,1) = A*0.5*omega0 - A*v(4) - 2*v(2)*v(4)/v(1) ...
    + (3/4)*R*omega0*v(2)/v(1);

end
```

Appendix C

MATLAB code for the solution to the Maxey-Riley equation using source-sink pair flow field

```
%This script is designed to solve the Maxey-Riley equation for a particle
%in the velocity field of a a source-sink pair in a constant flow
%Script name: covid_nonDim
%Author: Ajayi Olayinka Josiah


U= 2.9250;%m/sCharacteristic velocity
L= 0.65;%m Distance of sink from source (Source is located at the origin).
%L is also characteristic length
time= [0 10000000]*U/L;
Q= 1;%m2/sThis is the dimensional flow rate for the source
Q1= Q/(L*U); %This has been nondimensionalized
u0= 0;%m/s dimensional Velocity of constant flow
k_= 10;%m/s The velocity of interest where the particle starts from
k= k_/U;%This the nondimensional k
gamma= u0/U;%This has been nondimensionalized
lambda= Q1/(2*pi);
gy= 0;%m/s2 downward gravitational pull
g= [0 -gy]*L/U^2;%This value has been nondimensionalized.
%Gravity is currently off

rho_p= 1000;%kg/m3 At room temperature
rho_f= 1.184;%kg/m3 At room temperature
a= 10e-6;%m radius of aerosol
nu= 1.562e-5;%m2/s kinematic viscosity of fluid
Re= U*L/nu;%Reynolds number
St= (2/9)*(a/L)^2*Re;%Stokes number
R= 1.5;%2*rho_f/(rho_f + 2*rho_p);%When R= 2/3,<2/3 or >2/3, the particle is buoyant,
%heavy or light respectively
A= R/St;%Stokes drag
beta= 3;%Ratio of sink to source

amount= 21;%Number of particles captured
```

```
count=0;
for theta= linspace(0,2*pi,amount)
    count= count + 1;
    %Below is the initial point and velocity
    x1=cos(theta)*lambda/k;
    x2=sin(theta)*lambda/k;
    v1= gamma + lambda*(x1/(x1^2 + x2^2) - beta*(x1 - 1)/(x2^2 + (x1 -...
        1)^2));
    v2= lambda*(x2/(x1^2 + x2^2) - beta*x2/(x2^2 + (x1 - 1)^2));

    x0= [x1,v1,x2,v2]';%Intial position and velocity
    G= @(t,x) [x(2); (3*R*((gamma + lambda*(x(1)/(x(1)^2 + x(3)^2) - ...
        beta*(x(1) - 1)/(x(3)^2 + (x(1) - 1)^2)))*lambda*(1/(x(1)^2 + ...
        x(3)^2) - 2*x(1)^2/(x(1)^2 + x(3)^2)^2 - beta/(x(3)^2 + (x(1) - 1)^2)...
        + beta*(x(1) - 1)*(2*x(1) - 2)/(x(3)^2 + (x(1) - 1)^2)^2) + lambda^2*...
        (x(3)/(x(1)^2 + x(3)^2) - beta*x(3)/(x(3)^2 + (x(1) - 1)^2))*(-2*x(1)*...
        x(3)/(x(1)^2 + x(3)^2)^2 + 2*beta*(x(1) - 1)*x(3)/(x(3)^2 + (x(1) ...
        - 1)^2)^2)))/2 - A*x(2) + A*(gamma + lambda*(x(1)/(x(1)^2 + x(3)^2)...
        - beta*(x(1) - 1)/(x(3)^2 + (x(1) - 1)^2))) + (1 - (3*R)/2)*g(1); x(4);...
        (3*R*((gamma + lambda*(x(1)/(x(1)^2 + x(3)^2) - beta*(x(1) - 1)/(x(3)^2 ...
        + (x(1) - 1)^2)))*lambda*(-2*x(1)*x(3)/(x(1)^2 + x(3)^2)^2 + beta*x(3)...
        *(2*x(1) - 2)/(x(3)^2 + (x(1) - 1)^2)^2) + lambda^2*(x(3)/(x(1)^2 ...
        + x(3)^2) - beta*x(3)/(x(3)^2 + (x(1) - 1)^2))*(1/(x(1)^2 + x(3)^2)...
        - 2*x(3)^2/(x(1)^2 + x(3)^2)^2 - beta/(x(3)^2 + (x(1) - 1)^2) ...
        + 2*beta*x(3)^2/(x(3)^2 + (x(1) - 1)^2)^2)))/2 - A*x(4) ...
        + A*lambda*(x(3)/(x(1)^2 + x(3)^2) - beta*x(3)/(x(3)^2 ...
        + (x(1) - 1)^2)) + (1 - (3*R)/2)*g(2) ];
    [t,x]= ode15s(@(t,x) G(t,x),time,x0);%This is the solution to the
    %Maxey-Riley equation
    if count==3%This function solves for the saddle point
        fun= @(xx) [xx(2); (3*R*((gamma + lambda*(xx(1)/(xx(1)^2 ...
            + xx(3)^2) - beta*(xx(1) - 1)/(xx(3)^2 + (xx(1) - 1)^2)))...
            *lambda*(1/(xx(1)^2 + xx(3)^2) - 2*xx(1)^2/(xx(1)^2 + xx(3)^2)^2 ...
            - beta/(xx(3)^2 + (xx(1) - 1)^2) + beta*(xx(1) - 1)*(2*xx(1) - 2)/...
            (xx(3)^2 + (xx(1) - 1)^2)^2) + lambda^2*(xx(3)/(xx(1)^2 + xx(3)^2) ...
            - beta*xx(3)/(xx(3)^2 + (xx(1) - 1)^2))*(-2*xx(1)*xx(3)/(xx(1)^2 ...
            + xx(3)^2)^2 + 2*beta*(xx(1) - 1)*xx(3)/(xx(3)^2 + (xx(1) - ...
            1)^2)^2)))/2 - A*xx(2) + A*(gamma + lambda*(xx(1)/(xx(1)^2 + xx(3)^2)...
            - beta*(xx(1) - 1)/(xx(3)^2 + (xx(1) - 1)^2))) + (1 - (3*R)/2)*g(1);...
            xx(4); (3*R*((gamma + lambda*(xx(1)/(xx(1)^2 + xx(3)^2) - beta*(xx(1)...
            - 1)/(xx(3)^2 + (xx(1) - 1)^2)))*lambda*(-2*xx(1)*xx(3)/(xx(1)^2 ...
            + xx(3)^2)^2 + beta*xx(3)*(2*xx(1) - 2)/(xx(3)^2 + (xx(1) - 1)^2)^2)...
            + lambda^2*(xx(3)/(xx(1)^2 + xx(3)^2) - beta*xx(3)/(xx(3)^2 + (xx(1)...
            - 1)^2))*(1/(xx(1)^2 + xx(3)^2) - 2*xx(3)^2/(xx(1)^2 + xx(3)^2)^2 ...
            - beta/(xx(3)^2 + (xx(1) - 1)^2) + 2*beta*xx(3)^2/(xx(3)^2 + (xx(1) ...
            - 1)^2)^2)))/2 - A*xx(4) + A*lambda*(xx(3)/(xx(1)^2 + xx(3)^2)...
            - beta*xx(3)/(xx(3)^2 + (xx(1) - 1)^2)) + (1 - (3*R)/2)*g(2) ];
        epsilon= 0.01;%This is the solution for the saddle point
        %with an initial guess
        saddle = fsolve(fun,[-epsilon 1 0 1]);
    end
    plot(x(:,1),x(:,3),'-k')
    hold on
end
plot(0,0,'*b',1,0,'*r',saddle(1),saddle(3),'xk')
```

```
axis equal
axis([-0.8 1.2 -0.6 0.6])
xlabel('x-axis')
ylabel('y-axis')
title("R= "+ R +", St= "+ St +...
    ", \beta= "+ beta + ", \gamma = "+gamma + ", |g|= "+ abs(g(2)))
```

Bibliography

[1] A.A. Aleksandrov and M.S. Trakhtengerts. Viscosity of water at temperatures of- 20 to 150° c. *Journal of engineering physics*, 27(4):1235–1239, 1974.

[2] G.K. Batchelor. *An Introduction to Fluid Dynamics*. Cambridge University Press, 2000.

[3] Laurence Bergougnoux, Gilles Bouchet, Diego Lopez, and Elisabeth Guazzelli. The motion of solid spherical particles falling in a cellular flow field at low stokes number. *Physics of Fluids*, 26(9):093302, 2014.

[4] F. Candelier, J.R. Angilella, and M. Souhar. On the effect of the boussinesq–basset force on the radial migration of a stokes particle in a vortex. *Physics of Fluids*, 16(5):1765–1776, 2004.

[5] Christopher Yu Hang Chao, Man Pun Wan, Lidia Morawska, Graham R. Johnson, Z.D. Ristovski, Megan Hargreaves, K. Mengersen, S. Corbett, Yuguo Li, Xiaojian Xie, et al. Characterization of expiration air jets and droplet size distributions immediately at the mouth opening. *Journal of Aerosol Science*, 40(2):122–133, 2009.

[6] Kwitae Chong. *Particle Manipulation in Viscous Streaming*. PhD thesis, UCLA, 2013.

[7] John H. Costello and S.P. Colin. Morphology, fluid motion and predation by the scyphomedusa aurelia aurita. *Marine Biology*, 121(2):327–334, 1994.

[8] Lemuel M. Diamante and Tianying Lan. Absolute viscosities of vegetable oils at different temperatures and shear rate range of 64.5 to 4835 s- 1. *Journal of Food Processing*, 2014, 2014.

[9] Mohammad Farazmand and George Haller. The maxey–riley equation: Existence, uniqueness and regularity of solutions. *Nonlinear Analysis: Real World Applications*, 22:98–106, 2015.

[10] Aurelie Goater and Gregory A. Lawrence. Dispersion of heavy particles in an isolated pancake-like vortex. *Journal of Environmental Engineering and Science*, 3(5):403–411, 2004.

[11] Mahesh Jayaweera, Hasini Perera, Buddhika Gunawardana, and Jagath Manatunge. Transmission of covid-19 virus by droplets and aerosols: A critical review on the unresolved dichotomy. *Environmental Research*, 188:109819, 2020.

[12] Gabriel Provencher Langlois, Mohammad Farazmand, and George Haller. Asymptotic dynamics of inertial particles with memory. *Journal of nonlinear science*, 25(6):1225–1255, 2015.

[13] The Mathworks, Inc., Natick, Massachusetts. *MATLAB version 9.3.0.713579 (R2017b)*, 2017.

[14] Martin R. Maxey and James J. Riley. Equation of motion for a small rigid sphere in a nonuniform flow. *The Physics of Fluids*, 26(4):883–889, 1983.

[15] M.R. Maxey. The motion of small spherical particles in a cellular flow field. *The Physics of fluids*, 30(7):1915–1928, 1987.

[16] Efstathios E. Michaelides. A novel way of computing the basset term in unsteady multiphase flow computations. *Physics of Fluids A: Fluid Dynamics*, 4(7):1579–1582, 1992.

[17] Efstathios E. Michaelides. The transient equation of motion for particles, bubbles, and droplets. *Journal of fluids engineering*, 119(2):233–247, 1997.

[18] J. Peng and J.O. Dabiri. Transport of inertial particles by lagrangian coherent structures: application to predator-prey interaction in jellyfish feeding. *Journal of Fluid Mechanics*, 623:75–84, 2009.

[19] S Ganga Prasath, Vishal Vasan, and Rama Govindarajan. Accurate solution method for the maxey–riley equation, and the effects of basset history. *Journal of Fluid Mechanics*, 868:428–460, 2019.

[20] N. Raju and E. Meiburg. Dynamics of small, spherical particles in vortical and stagnation point flow fields. *Physics of Fluids*, 9(2):299–314, 1997.

[21] Vincent Rossi, Pedro Monroy, Cristobal López, Emilio Hernández-García, Boris Dewitte, Aurélien Paulmier, and Véronique Garçon. Modeling the dynamical sinking of biogenic particles in eastern-boundary upwelling systems. *EGUGA*, page 14468, 2017.

[22] Boris M. Smirnov and R. Stephen Berry. Growth of bubbles in liquid. *Chemistry Central Journal*, 9(1):48, 2015.

[23] Senbagaraman Sudarsanam. *Inertial Particle Dynamics In Simple Vortex Flow Configurations*. PhD thesis, Clemson University, 2015.

[24] Julian W Tang, Andre D Nicolle, Christian A Klettner, Jovan Pantelic, Liangde Wang, Amin Bin Suhaimi, Ashlynn Y.L. Tan, Garrett W.X. Ong, Ruikun Su, Chandra Sekhar, et al. Airflow dynamics of human jets: sneezing and breathing-potential sources of infectious aerosols. *PLoS One*, 8(4):e59970, 2013.

[25] C.M. Tchen. *Mean Value and Correlation Problems Connected with the Motion of Small Particles in a Turbulent Fluid*. PhD thesis, University of Delft, 1947.

[26] Marco Thiel, Jürgen Kurths, M. Carmen Romano, György Károlyi, and Alessandro Moura. *Nonlinear dynamics and chaos: advances and perspectives*. Springer, 2010.

[27] Y.S. Touloukian and T. Makita. Thermophysical properties of matter-the tprc data series. volume 6. specific heat-nonmetallic liquids and gases. Technical report, THERMOPHYSICAL AND ELECTRONIC PROPERTIES INFORMATION ANALYSIS CENTER, 1970.